RESEARCH ARTICLE

High genome plasticity and frequent genetic exchange in *Leishmania tropica* isolates from Afghanistan, Iran and Syria

Hedvig Glans[1,2]*, **Maria Lind Karlberg**[3], **Reza Advani**[3], **Maria Bradley**[2,4], **Erik Alm**[5], **Björn Andersson**[6], **Tim Downing**[7]

1 Department of Infectious Diseases, Karolinska University Hospital, Stockholm, Sweden, **2** Division of Dermatology & Venerology, Dept of Medicine Solna, Karolinska Institutet, Stockholm, Sweden, **3** Department of Microbiology, The Public Health Agency of Sweden, Stockholm, Sweden, **4** Department of Dermatology and Venerology, Karolinska University Hospital, Stockholm, Sweden, **5** The European Center for Disease Prevention and Control, Stockholm, Sweden, **6** Department of Cell & Molecular Biology, Karolinska Institutet, Stockholm, Sweden, **7** School of Biotechnology, Dublin City University, Dublin, Ireland

* hedvig.glans@ki.se

Abstract

Background

The kinetoplastid protozoan *Leishmania tropica* mainly causes cutaneous leishmaniasis in humans in the Middle East, and relapse or treatment failure after treatment are common in this area. *L. tropica*'s digenic life cycle includes distinct stages in the vector sandfly and the mammalian host. Sexual reproduction and genetic exchange appear to occur more frequently than in other *Leishmania species*. Understanding these processes is complicated by chromosome instability during cell division that yields aneuploidy, recombination and heterozygosity. This combination of rare recombination and aneuploid permits may reveal signs of hypothetical parasexual mating, where diploid cells fuse to form a transient tetraploid that undergoes chromosomal recombination and gradual chromosomal loss.

Methodology/principal findings

The genome-wide SNP diversity from 22 *L. tropica* isolates showed chromosome-specific runs of patchy heterozygosity and extensive chromosome copy number variation. All these isolates were collected during 2007–2017 in Sweden from patients infected in the Middle East and included isolates from a patient possessing two genetically distinct leishmaniasis infections three years apart with no evidence of re-infection. We found differing ancestries on the same chromosome (chr36) across multiple samples: matching the reference genome with few derived alleles, followed by blocks of heterozygous SNPs, and then by clusters of homozygous SNPs with specific recombination breakpoints at an inferred origin of replication. Other chromosomes had similar marked changes in heterozygosity at strand-switch regions separating polycistronic transcriptional units.

Conclusion/significance

These large-scale intra- and inter-chromosomal changes in diversity driven by recombination and aneuploidy suggest multiple mechanisms of cell reproduction and diversification in *L. tropica*, including mitotic, meiotic and parasexual processes. It underpins the need for more genomic surveillance of *Leishmania*, to detect emerging hybrids that could spread more widely and to better understand the association between genetic variation and treatment outcome. Furthering our understanding of *Leishmania* genome evolution and ancestry will aid better diagnostics and treatment for cutaneous leishmaniasis caused by *L.tropica* in the Middle East.

Author summary

Cutaneous leishmaniasis is mainly caused by *Leishmania tropica* in the Middle East, where it is known for treatment failure and a need for prolonged and/or multiple treatments. Several factors affect the clinical presentation and treatment outcome, such as host genetic variability and specific immune response, as well as environmental factors and the vector species. Little is known about the parasite genome and its influence on treatment response. By analysing the genome of 22 isolates of *L. tropica*, we have revealed extensive genomic variation and a complex population structure with evidence of genetic exchange within and among the isolates, indicating a possible presence of sexual or parasexual mechanisms. Understanding the *Leishmania* genome better may improve future treatment and better understanding of treatment failure and relapse.

Introduction

Leishmaniasis is a vector-borne parasitic disease transmitted by sand flies. At least twenty *Leishmania* species are pathogenic to humans and can cause a spectrum of clinical manifestations, from chronic local ulcers to cutaneous leishmaniasis (CL), and to infection of internal organs in visceral leishmaniasis [1–3]. Host genetic variability, host immune responses, sand fly feeding behaviour, environmental factors and parasite species and strain variation all influence the clinical manifestation and the outcome of the infection [4]. Genome sequencing within *Leishmania* species has mostly shown a lack of a clear association between genetic differences and the clinical pathology [5].

 L. tropica is a heterogeneous species complex with a broad geographical distribution across Africa and Eurasia [3,6,7] that causes mainly CL, though visceral leishmaniases has been reported [8,9]. *L. tropica* is typically an anthroponotic disease, though zoonotic transmission may be possible as well [10–12]. Although the burden of leishmaniasis is decreasing globally, regions with *L. tropica* have increasing rates due to local conflicts and associated population displacement, migration and relocation [3], which exacerbates incorrect CL diagnoses and inadequate access to appropriate healthcare and treatments. CL caused by *L. tropica* in the Middle East can be difficult to treat: lesions may relapse (called leishmaniasis recidivans) and multiple or prolonged treatments are often necessary [13,14].

 Leishmania have specific *Phlebotomine* sandfly vector compatibilities that affect transmission [15,16]. In most geographic areas, *L. tropica* is transmitted by its most common vector, the female *Phlebotomus sergenti* sandfly [17]. Although other vectors like *P. arabicus* in

northern Israel [18] and *P. guggisbergi* in Kenya [19] also are known. *Phlebotomus spp.* can be infected by different *Leishmania spp.*, including *P. perniciosus* [20], *P. tobbi* by *L. tropica* and *L. infantum* [20,21] and *P. guggisbergi* by *L. tropica* and *L. major* [19]. Hybrids capable of transmitting have formed in all these vectors [22]. *L. tropica*'s digenic life cycle has an extracellular promastigote stage where they occupy different regions of the alimentary tract of the vector, and subsequently as amastigotes within mammalian macrophages [23]. During the extracellular growth and development in the vector, *Leishmania* is capable of non-obligatory meiotic genetic exchange [24].

Evidence of hybridisation has been observed in diverse natural isolates of *Leishmania* [25–28] and in culture [29]. It is possible but still uncertain that reproduction in *Leishmania* could be facilitated by genes with high similarity to ones involved in meiosis [24] to allow crossing-over, resulting in recombinant chromosomes [30]. As more *Leishmania* are genetically profiled, the precise mechanisms involved and frequencies of *Leishmania* meiotic or quasi-sexual events are beginning to become clearer. Classical meiosis like that of the related kinetoplastid *Trypanosoma brucei* [31] has not been observed in *Leishmania*-infected sand flies, but there is indirect evidence that it does occur [32]. Although the universal mosaic aneuploidy of *Leishmania* is inconsistent with classical meiosis, experimental backcrosses can produce hybrids in sand flies with varying degrees of genetic relatedness among parental lines [32]. Possible alternative mechanisms like parasexual reproduction have been considered for *Leishmania* based on observations in *Saccharomyces* [32], such as a tetraploid meiotic cycle in which diploid parental cells fuse followed by a meiosis, resulting in diploid F1 [32]. Another model is parasexual reproduction in which a fusion of parental cells is followed by karyogamy, re-shuffling of DNA regions, and gradual loss of chromosome copies during mitoses [24,29,30,33]. There is evidence for this in experimental *L. major* and *L. infantum* crosses [34] and *Trypanosoma cruzi* [31,35]. These mechanisms are not mutually exclusive, and different types of genetic exchange are possible [35,36].

Leishmania hybrids generated *in vitro* and in sand flies are mostly diploid at the time of culturing and contain approximately equal amounts of genetic material from both parental strains [32,37], suggesting meiosis-like processes. Triploid and tetraploid hybrid offspring have also been observed, which could indicate other mechanisms [24,29,37]. Genome sequencing of triploid hybrids indicated that a triploid F1 (3n) may be a product of fusion between a diploid cell that failed to undergo meiosis (2n) and a haploid cell (1n) [37]. Hybrid strains have been generated experimentally with different *Leishmania spp.* in sand flies, both within and between species [27,32,38–40]. Natural hybrid isolates have been found in a range of geographical settings, suggesting abundant natural genetic exchange within and between different species that is important for the evolution of the parasite [25–27,41–43] to enhance transmission potential and increase the fitness of the parasites [29,32,34,44]. *Leishmania* genomes are unstable and lack promoter-dependent gene regulation [45]. Together with post-transcriptional regulations, *Leishmania* exploits gene dosage by chromosome and gene copy number variation [46–48] which are driven by variable environments that maintain expression levels and genetic diversity [49]. Thus, inter-species hybrids may have facilitated the spread of *Leishmania* to new geographic regions through changes in vector specificity [16]. Although new interspecies hybrids are usually not able to carry out genetic exchange, intra-species hybrids could produce new progeny. The ability to produce hybrids *in vitro* and *in vivo* varies between species: it is lower in *L. major* [24,37] than *L. tropica*, where a higher frequency of hybrid formation in co-infected sand flies has been observed [32].

Leishmania possesses universal aneuploidy in natural isolates, laboratory strains, in experimental hybrids and during culture [32,50–52]. This mosaic aneuploidy is primarily a result of mitotic asymmetric chromosome allotments [30]. This enhances the genomic variation

through differences in gene copy numbers and chromosomal duplication events [47,53]. Aneuploidy may facilitate eliminating deleterious mutations during chromosome loss, and the persistence of an intra-strain genetic heterogeneity may be beneficial for the cell population [54].

In *Leishmania*, there may be only one single region per chromosome where DNA replication initiation occurs, detected during the S phase [55]. This may lead to incomplete duplication of the larger chromosomes during S phase and an inadequate duplication of the genome prior to cell division [55]. *Leishmania* employs sub-telomeric DNA replication beyond S phase, which may be less effective in maintaining genome integrity, and in this way contributes to variability and aneuploidy [56].

Gene expression in *Leishmania* is carried out through polycistronic transcriptional units (PTUs) [57] separated by strand-switch regions (SSRs) where RNA polymerase II can transcribe bidirectionally [58]. Genes are transcribed as multigene pre-mRNAs with a single constitutive transcription start site (TSS) [58,59] and are trans-spliced to form mature mRNAs. This means gene dosage is crucial [46, 60] since gene regulation is mostly post-transcriptional [61,62], leading to both intra- and extrachromosomal genome-wide gene copy number variation and mosaic aneuploidy. *L. tropica* has high levels of allelic diversity and heterozygosity, consistent with frequent full genome-hybridization, most likely due to natural outcrossing [32,63].

Despite previous research in the field, much remains unclear regarding the diversity, evolution, and genetic exchange of *L. tropica*. In this study, we have investigated 22 isolates of *L. tropica* from 21 patients, focusing on the genetic diversity within and between the isolates and correlating the results to their geographic sources in Afghanistan, Iran and Syria. The study revealed large-scale intra- and inter-chromosomal changes in diversity driven by recombination and aneuploidy that enhance our understanding of *Leishmania* genome evolution and ancestry.

Methods

Ethics statement

Ethical approval was obtained from the Central Ethical Review Board in Stockholm (2015/2162–31). Informed consent was not found to be necessary, as the samples, included in the genome study, and the clinical data were anonymized, and only isolated parasites were studied.

Sample collection

The *L. tropica* isolates were sampled from 21 patients diagnosed with CL in 2007–2017. The patients were from Syria (17), Afghanistan (3) and Iran (2). The patients were treated with sodium stibogluconate (7), cryotherapy (5), liposomal amphotericin (5), meglumine antimoniate (2), fluconazole (1), cryotherapy and sodium stibogluconate (1), cryotherapy and liposomal amphotericin (1), or had no treatment (2) (Table 1). One patient with leishmaniasis recidivans had not visited endemic areas since first symptoms of CL, was first sampled in 2014 followed with a second sample in 2017 after ineffective sodium stibogluconate treatment, resulting in 22 *Leishmania* genomes for investigation.

Culturing, DNA extraction, library preparation and short read sequencing

The isolates were stored at -156˚C at the Public Health Agency of Sweden. Promastigotes were cultivated in RMPI 1640 medium with L-Glutamin, HEPES, Penicillin-Streptomycin and fetal

Table 1. 21 patients with 22 isolates of *L. tropica* (* from the same patients) infected in the Middle East (three from Afghanistan, two from Iran, 17 from Syria). Ten had received treatment prior sampling (nine SSG, one cryotherapy) and twelve were cured on first-line treatment after sampling. Six were cured on second-line treatment (3 LA, 3 SSG il). One healed by itself and two were lost after sampling. One patient continued to relapse regarding treatment. ** healed by itself. SSG stands for sodium stibogluconate, LA for liposomal amphotericin, MA for meglumine antimoniate, il for intralesional, im for intramuscular, iv for intravenous, cured for absence of clinical relapse for 6 months after treatment, relapse for recurrence of a lesion after the lesion had healed without any known new exposure to the parasite, treatment failure for absence of clinical signs of re-epithelialisation in the lesion during or within two months after treatment.

Sample ID	Country	Previous treatment	Treatment	First-line treatment	Treatment outcome	Second-line treatment	Treatment outcome
07_00242	Iran	Yes	SSG	No treatment	Cured		
07_01513	Syria	No		NA			
13_00550	Syria	Yes	SSG	SSG iv	Cured		
13_01024	Syria	No		Cryotherapy	Cured		
13_01233	Afghanistan	No		Cryotherapy	Cured		
13_01390	Syria	Yes	SSG	SSG iv	Relapse	LA	Cured
14_00642	Syria	No		SSG iv	Relapse	LA	Cured
14_00771	Syria	Yes	SSG	LA	Cured		
14_00849	Syria	No		MA im	Cured		
14_01223*	Syria	Yes	SSG	SSG iv	Treatment failure	LA	Cured
15_00019	Syria	Yes	SSG	LA	NA		
15_01088	Syria	Yes	SSG	SSG il	Cured		
15_01620	Syria	No		LA	Treatment failure	SSG iv	Cured
15_02015	Syria	No		MA im	Cured		
15_02480	Afghanistan	No		Fluconazole	Treatment failure	LA	Treatment failure**
15_02576	Syria	No		Cryotherapy	Cured		
15_02597	Syria	Yes	Cryotherapy	Cryotherapy	Treatment failure	SSG il	Cured
16_00075	Afghanistan	No		LA + Cryotherapy	Treatment failure	SSG il	Cured
16_00674	Syria	No		LA	Cured		
16_00964	Iran	No		SSG il + Cryotherapy	Cured		
16_14706	Syria	Yes	SSG	Cryotherapy	Cured		
17_01604*	Syria	Yes					

calf serum at 23°C [64]. All isolates were grown for the minimum time necessary to produce adequate parasite numbers to isolate enough genomic DNA (gDNA) for library preparation. A QIAamp Mini Kit (QIAGEN) was used to extract DNA, and Qubit dsDNA BR Assay Kit (Invitrogen, Thermo Fisher Scientific, USA) was used to measure DNA concentrations—all according to manufacturer's protocols. 200 ng gDNA was used for library construction using the Ion Xpress Plus Library Kit following the manufacturer's instruction. The libraries were quantified by an in-house qPCR, MGB (minor groove binder) assay [65]. For template preparation, gDNA libraries were pooled to a final concentration of 30 or 50 pM and clonally amplified using the Ion Torrent Chef system using the Ion 510&520&530 Kit-chef or Ion 540 Kit-chef and then loaded onto an Ion 530 or 540 chip, respectively. Massively parallel sequencing was then performed on an IonTorrent S5 XL instrument (Thermo Fisher Scientific, USA) according to the manufacturer's protocol. The template preparation and sequencing were repeated for each sample until the initial obtained sequencing data corresponded to more than >30x genome-wide coverage.

Read processing, mapping and SNP screening

Sequencing of the libraries resulted in an average of 8.73±4.40 (mean±SD) million single-end raw reads of up to 557 bp in length, with at least 4.14 million raw reads per sample. The quality of the initial DNA read libraries varied considerably, and careful quality control was conducted

to ensure only high-quality reads were retained and low-quality reads were discarded (S1 Table). The reads were trimmed including removal of adaptor sequence using the Torrent Suite software with standard settings (Torrent suite v5.2.2) (SRA accession PRJEB45563) resulting in 22 valid short read libraries. Remaining low-quality bases with a base quality <30 were removed with the FASTX-Toolkit v0.0.14 (http://hannonlab.cshl.edu/fastx_toolkit/), and the absence of remaining low-quality reads was verified with FastQC v0.11.5 (www.bioinformatics.babraham.ac.uk/projects/fastqc/). These high-quality reads had lengths of 70–557 bases after screening and an average of 6.98±2.58 million reads per sample (S1 Table).

'The reference genome used for analyses was the *L. tropica* LRC-L590 (MHOM/IL/1990/P283) assembly v2.0.2 with annotation from Companion [66] accessed through the Sanger Institute. It was masked using Tantan v13 [67] to exclude repetitive sequences, short tandem repeats, homopolymers and low-quality regions. The screened reads were mapped to this reference with Smalt v7.6 (http://www.sanger.ac.uk/science/tools/smalt-0) with a k-mer length of 19 so that candidate variants could be determined. Initial candidate SNPs (278,616±25,792) were extracted using BCFtools v1.10.2 [68] from which valid SNPs were selected that had base quality >25, mapping quality >30, >4 forward derived alleles, >4 reverse derived alleles, and read coverage >10-fold. This was visualised for each parameter with RStudio v4.0 across the collection (S1 Fig). Regions with 100 bases of the chromosome edges were excluded. This resulted in a total of 301,659 valid SNPs across all samples, with 170,183±63,717 SNPs per library across the genome, with at least 69,843 SNPs per sample (S1 Table). Excluding contigs not assigned to chromosomes, this meant 169,753±63,717 valid SNPs per sample, with an average of 430±186 valid SNPs on contigs. The association between the numbers of initial reads and candidate SNPs was high (r^2 = 0.243) compared to the association between the numbers of valid reads and valid SNPs (r^2 = 0.028), suggesting that quality-control improved the accuracy of the true variation present. After careful checking, there were 17 mutations at 11 SNPs that were triallelic SNPs where both derived alleles were observed, based on derived allele frequencies <0.9 and read depth >14. SNP density measurements assumed a quasi-Normal distribution across the chromosomes based on Shapiro-Wilk normality tests excluding outlying chromosomes with extreme SNP rates.

De novo assembly

Each read library (except 13_01024) was assembled *de novo* for all k-mer lengths from 33 to 253 inclusive with a step size of 10 bases with Megahit v1.2.9 [69], retaining contigs of >1 Kb. This optimised the assembly using de Bruijn graph information from different k-mers and can cope well with heterogeneous data whose local copy numbers and read depths varied [69]. Here, it was used to verify large structural rearrangements and has been previously used on *Leishmania* genomes [70]. These initial *de novo* assemblies had an average of 8,152±3,025 contigs with an average N50 of 7,816±3,218. They were contiguated using the *L. tropica* reference with ABACAS [71] to produce assemblies whose chromosomes spanned 32.85±0.94 Mb excluding N bases, which was similar to the reference's length (32.93 Mb). A comparison of the Z-normalised reference chromosome lengths to the Z-normalised *de novo* ones for all samples indicated that few chromosomes had extreme differences in lengths after Benjamini-Hochberg (BH) p value correction. However, lengths were longer than expected for chromosome 7 for 14_00771 (p = 0.022) and 15_0215 (p = 0.038), and several other chromosomes noted when discussed below.

Long read sequencing, assembly and SNP screening

PacBio long read sequencing of 13_00550 produced 1.05 billion bases across 68,806 reads with a mean length of 15,225 bases and a N50 of 33,952. After quality control and mapping, 64,437

high-quality reads resulted in an average of 40-fold coverage across the *L. tropica* reference genome. After assembly and polishing by Hierarchical Genome Assembly Process 3 (HGAP3, [72]), the 13_00550 assembly had 2,655 contigs with a contig N50 of 19,171 spanning 32.7 Mb. This assembly masked with Tantan v13 as above and contiguated using the *L. tropica* reference with ABACAS [71] to produce an assembly whose chromosomes spanned 34,152,472 bp: 29,861,533 bp excluding N bases. This was indexed using Smalt v7.6 and reads for the 13_00550 short read library were mapped to it. After quality control and SNP calling as above using BCFtools v1.10.2, this found 21,663 heterozygous and zero homozygous SNPs across the chromosomes, supporting our SNP calling approach.

Inference of population structure and ancestry

Population structure was evaluated across the 301,659 SNPs by constructing a nuclear DNA maximum-likelihood phylogeny based on 168,327 alignment patterns using RAxML v8.2.11 with a GTR+gamma substitution model [73]. This was visualised with the *L. tropica* reference as an unrooted phylogeny using R packages ape v5.5 and phytools v0.7–70. To further resolve ancestries within discrete genomic chromosomes and regions, phylogenies per chromosome were constructed as above using RAxML v8.2.11 were visualised with phytools v0.7–70 and dendextend v1.14.0 [74].

We classified the 22 samples into genetically distinct groups using a hierarchical Bayesian clustering (BHC) with a Dirichlet Process Mixture model implemented in FastBAPS v1.0 [75]. This interpreted the SNP variation as a sparse matrix with an optimised hyperparameter of 0.092 for the genome-wide pattern using R packages ape v5.5, ggplot2 v2.3.3.3, ggtree v2.4.1 [76], phytools v0.7–70 and treeio v1.14.3. Isolates were allocated to genetically distinct groups per chromosome using FastBAPS v1.0 with a population mean prior and chromosome-specific optimised hyperparameters. This clustering was repeated for regions of interest on chromosomes 10, 12, 23, 29, 31 and 36.

Kinetoplast DNA variation

The kinetoplast DNA (kDNA) is a high copy number network of circular minicircle and maxicircle DNA molecules. The 22 libraries were mapped to the masked *L. tarentolae* reference maxicircle kDNA (20,992 bp, accession M10126.1, [77] using Smalt v7.6. The *L. tropica* reference maxicircle was tested, but the assembly quality of that contig limited any inferences. Valid SNPs were determined where the mapping quality > 30, the read-depth allele frequency (RDAF) > 0.8, and the read depth of high-quality reads > 10, excluding sites within 100 bp of the maxicircle reference ends. This found 1,594 SNPs distinguishing all of the 22 isolates from the *L. tarentolae* reference, which phylogenetically clustered most closely with isolate 13_01390. Within the 22 *L. tropica* isolates, there were 220 variable sites, with a frequency per sample ranging from 9 to 154 SNPs with an average of 82±39 SNPs. The variation was visualised with IGV v2.8.12 with the *L. tarentolae* annotation. A phylogeny was constructed as above using RAxML v8.2.11 with a GTR+CAT substitution model [73] and using R packages ape v5.5 and phytools v0.7–70. As above, genetically distinct groups were assigned using FastBAPS v1.0.

Aneuploidy and structural variation

Chromosomal somy levels were determined using the read depth coverage per base normalised by the median genomic coverage for each library [78] scaled as the haploid depth. This excluded sites at the first 7 Kb or last 2 Kb of chromosomes [79]. All libraries had at least 21-fold median genome-wide coverage except samples 13_01233 and 13_00550 whose median

coverage was 13-fold, so an alternative somy estimation using binning was not essential here. Read depth was determined from the mapping patterns for chromosomal regions using 5 Kb windows to account for local variability. This yielded power to examine large structural changes of >10 Kb: small structural variants and indels were not examined in detail here due to potential artefacts associated with the sequence quality.

Results

We isolated, sequenced and analysed 22 *L. tropica* isolates from infected patients originally from Afghanistan (n = 3), Iran (n = 2) and Syria (n = 17) to decipher processes driving genome evolution in this unique collection.

Genomic diversity and population structure in *L. tropica*

The analysis of the sequence data identified 301,659 SNPs across all sample including multi-allelic sites and 1,396 unique SNPs in contigs including multi-allelic sites. The isolates had differences in chromosomal diversity, with a range of 69,662 to 277,195 SNPs per isolate (SNPs on contigs were not examined in this study). Most SNPs were heterozygous: the number of homozygous SNPs per sample was 4,886±2,855, corresponding to 0.15 SNPs/Kb, with a range of 2,346 to 13,371. The number of heterozygous SNPs was much higher at 164,886±64,763 per sample, corresponding to 5.0 SNPs/Kb, with a range of 64,391 to 273,463. The numbers of homozygous and heterozygous chromosomal SNPs per sample had a small negative correlation ($r^2 = 0.07$, S2 Fig), suggesting processes other than genetic drift were contributing to the variation. We validated our careful sequencing, processing and SNP ascertainment approach by long PacBio read sequencing of isolate 13_00550. This resulted in zero genome-wide homozygous SNPs after self-mapping its own short reads to its *de novo* assembly, and high heterozygosity compared to when the reads were mapped to the *L. tropica* LRC-L590 reference genome.

Two genetically distinct groups were evident based on the patterns of a chromosome-wide phylogeny constructed with RAxML v8.2.11 [73] and population structure from FastBAPS v1.0 [75] (Fig 1). The first genetically distinct group (n = 7) was related to the *L. tropica* reference genome and hence is referred to as the reference group. The second (n = 15) was divergent from the reference genome and is here called the non-reference group. Isolates from Syria, Afghanistan and Iran were found in both groups. The two isolates from the same patient in Syria (14_01223 and 17_01604) were both from the non-reference group. Certain isolates with long external phylogenetic branches that were phylogenetically close to being between the two groups had instances of inconsistent group assignment by FastBAPS. For example, 12 out of the 36 chromosomes of 16_00964 were allocated to the reference group by FastBAPS and 24 to the non-reference genome group.

Independent infections in a single patient

The patient sampled twice, in 2014 (14_01223) and 2017 (17_01604), had both isolates taken from a large lesion (diameter 80 mm) at two different locations on the lesion. The patient received treatment between the sampling times but continued to relapse (leishmaniasis recidivans). These two isolates were genetically different from each other with no evidence of a mixed infection (Fig 1): 14_01223 and 17_01604 had 159,535 genome-wide SNPs between them, including 1,616 on chromosome 2, and 15,606 on chromosome 36 (Fig 2).

14_01223 and 17_01604 were both allocated to the same non-reference genetic group, but when examined individually 14_01223's chromosomes 2 and 36 were genetically related to the reference group. 14_01223 had long runs of homozygosity (LROHs) across all of chromosome
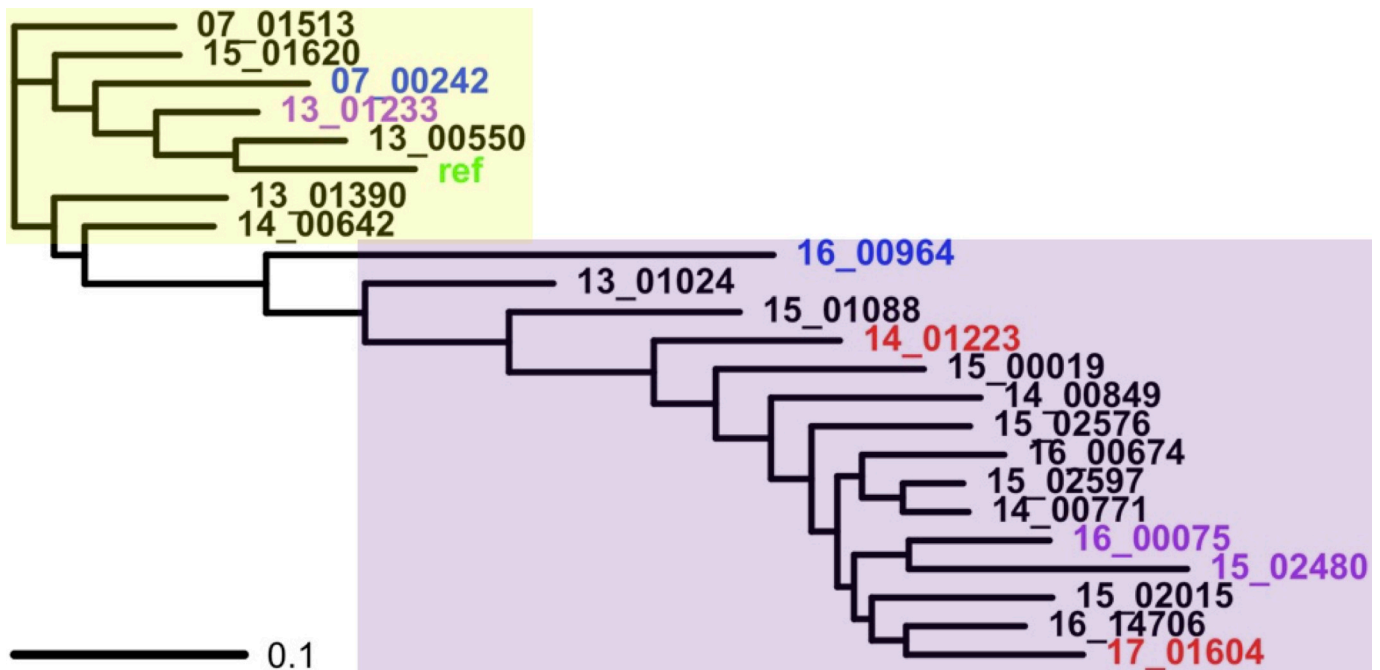
Fig 1. A phylogeny constructed from all chromosomal SNPs showing the relatedness of the 22 isolates with the *L. tropica* reference genome ("ref", green). The samples were from Syria (n = 17, black/red), Afghanistan (n = 3, purple) and Iran (n = 2, blue). Isolates 14_01223 and 17_01604 were from the same patient (red). The inferred genetically distinct groups from FastBAPS are represented by the *L. tropica* reference (yellow area) and non-reference groups (purple area).

2 and at chromosome 36 >1.63 Mb to the end at 2.715 Mb (Fig 2). In contrast, 17_01604 was heterozygous throughout. This difference in variation was confirmed by the SNPs' RDAF distributions which were skewed for 14_01223 but normal for 17_01604 (S3 and S4 Figs). The chromosome 36 of 14_01223 displayed heterozygosity at <1.63 Mb, then a LROH at 1.63–1.78 Mb, followed by near homozygosity >1.80 Mb. Based on inferred patterns from *L. major*, the 1.63 Mb breakpoint coincided with an acH3 mark, and the 1.78–1.80 Mb region corresponded with a putative transcription start site (TSS) near an inferred SSR. The patient had a mixed infection with two unique isolates, allocated to the non-reference genetic group, but with clear genomic differences.

Varied ancestry and heterozygosity at chromosome 36

Further examination of chromosome 36 in 14_01223 with 14_00642, 16_00075, 16_00964 and 07_00242 presented sharp homozygosity-heterozygosity switches (Fig 3). 07_00242 and 16_00964 had similar patterns like a change at an inferred SSR and putative acH3 mark at 1.42 Mb, where the pattern of heterozygosity changed to a LROH until 1.8 Mb, before moving to homozygous similarity (Fig 2). 16_00075 had a jump in the RDAF at 1.28 Mb (at acH3 and baseJ marks) before a RDAF drop at 1.75 Mb that was also in 14_00642—neither of these samples had LROHs. All these five samples were disomic for this chromosome, except for trisomy in 14_00642 (S4 Fig).

The heterozygous and homozygous SNP densities, phylogenetic patterns, FastBAPS population assignment (S5 Fig), and mean RDAF consistent with somy levels at 0–1.28 Mb of chromosome 36 matched the genome-wide patterns and main trends in other chromosomes (Fig 3). The region at 1.28–1.60 Mb was heterogeneous due to the higher number of potential recombination breakpoints (Fig 3). At 1.60–1.78 Mb, 14_01223, 07_00242 and 16_00964 had
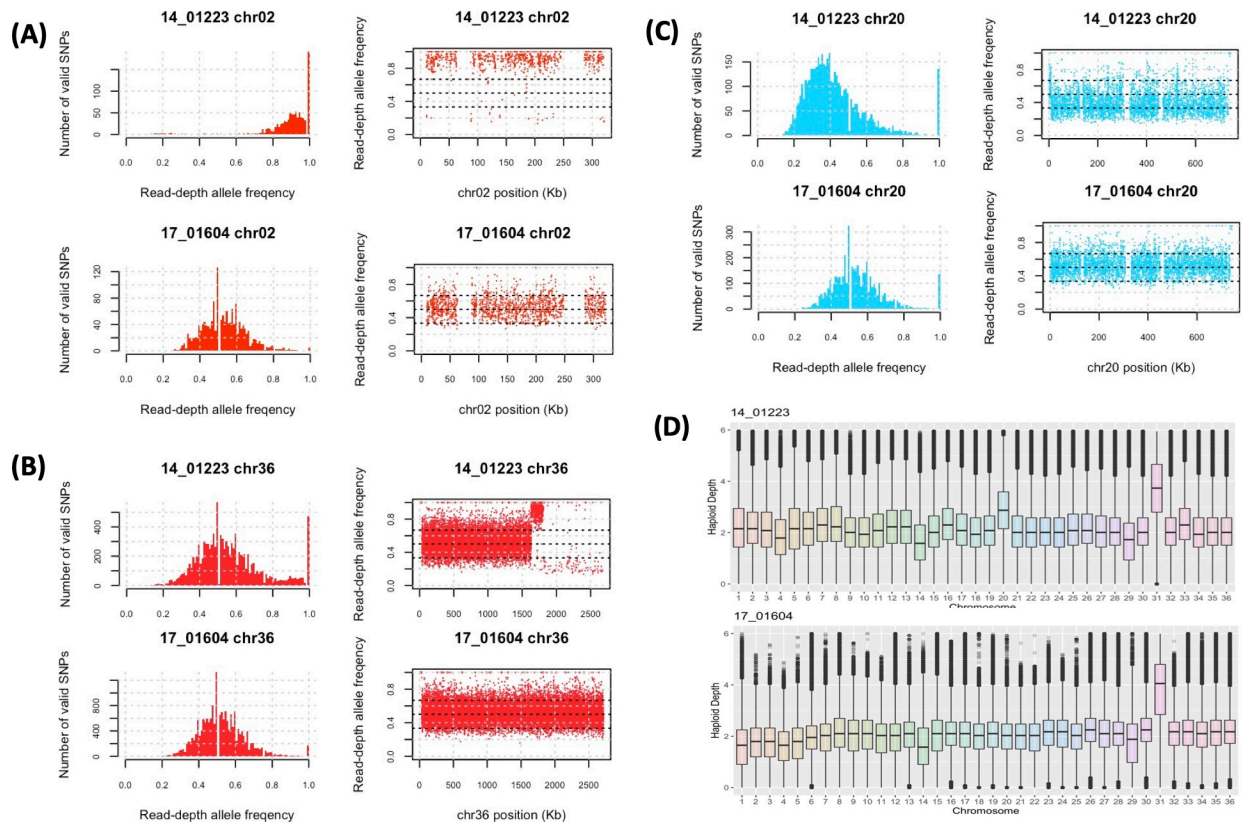
Fig 2. 14_01223 and 17_01604 were from the same patient originally from Syria but were genetically distinct. The genetic differences between these were illustrated by the SNP RDAF distributions (left of each panel) and the RDAF levels across the chromosome (right of each panel). (A) For chromosome 2, 14_01223 was nearly homozygous, whereas 17_01604 had heterozygosity comparable with most other samples (S3 Fig). (B) 14_01223 had a region with a high RDAF at 1.63–1.78 Mb followed by homozygosity at >1.80 Mb that 17_01604 did not have. (C) Chromosome 20 was approximately trisomic in 14_01223 but disomic in 17_01604 as shown by the RDAF distributions. (D) The haploid depth of each chromosome showed minimal differences except for chromosome 20.

LROHs, contrasting with the lower relative heterozygosity in the other 19 samples. Moreover, these three samples had unique ancestry (A) for this region, differentiating them from the expected reference (R) and non-reference (N) groups based on FastBAPS analysis (S5 Fig). This deviation in genetic ancestry continued for the rest of the chromosome, and all four strains were found to be related to the reference group, which was surprising for 07_00242, 16_00964 and 16_00075 had been assigned to the non-reference group at the whole-genome level. 16_00075 was unambiguously disomic for this chromosome, implying that the change in the main RDAF peak of ~0.5 at 0–1.28 Mb to a peak of ~0.75 at 1.28–1.75 Mb and then to ~0.25 at >1.75 Mb (S6 Fig) was a mix of cells with varied ancestries including a genetically different middle segment. Like all 22 samples here, 16_00075 was heterozygous at <1.28 Mb on this chromosome (R/N genotype). At >1.8 Mb, ~50% of 16_00075's cells were likely R/R, and ~50% were R/N, yielding a mean RDAF of ~0.25. In the middle at 1.28–1.75 Mb the other ancestry (A) implied a mosaic of R/A genotypes. The shift in pattern indicated a genetic exchange that may be the result of a sexual reproduction.

Consistent recombination breakpoints at tetrasomic chromosome 31

The *Leishmania* chromosome 31 often shows a pattern of tetrasomy and high heterozygosity and this was also observed here (S4 Fig), indicative of likely homologous recombination across
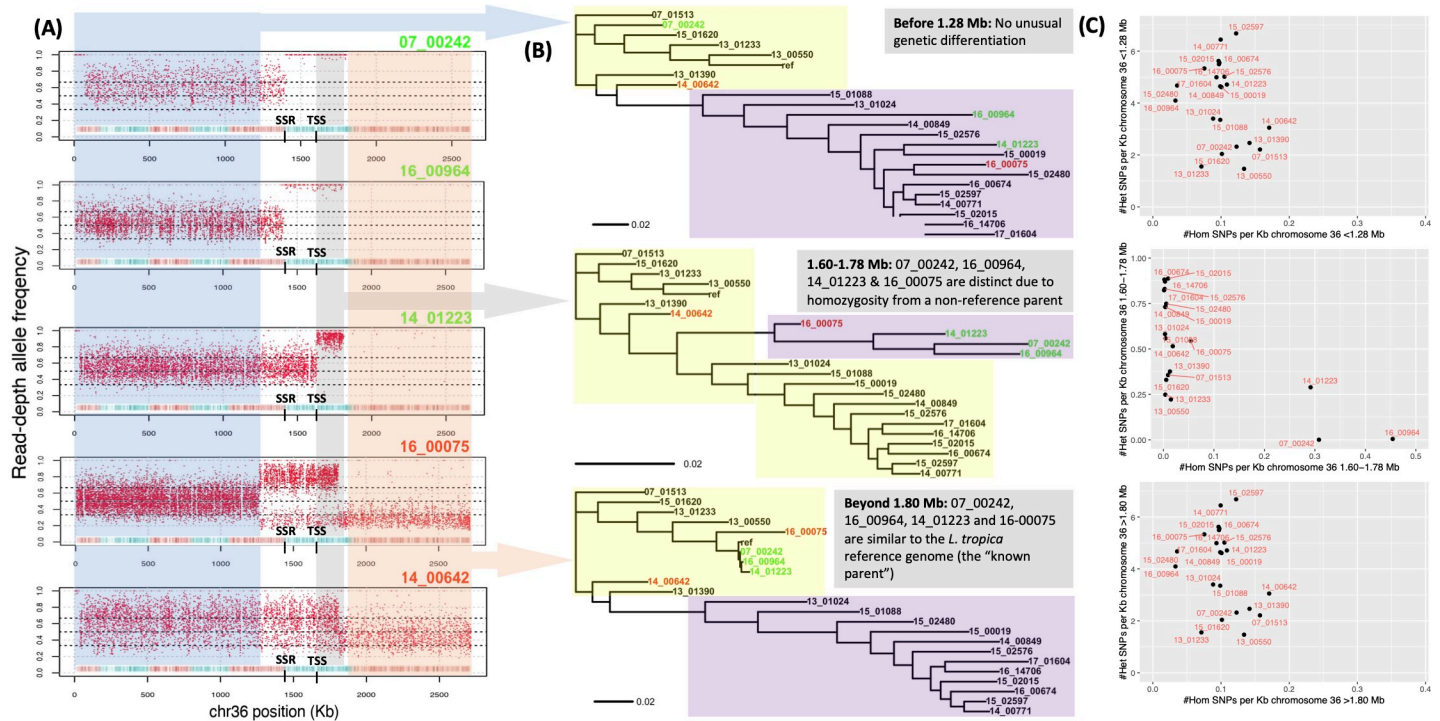
Fig 3. RDAF distributions (A) and phylogenies (B) constructed from SNPs at the 5'-end of chromosome 36 (<1280 Kb, blue RDAF, top phylogeny), middle (1600–1780 Kb, grey RDAF, middle phylogeny) and 3' end (>1800 Kb, orange RDAF, bottom phylogeny) showing the genetic relatedness of the 22 isolates with the *L. tropica* reference genome ("ref"). (A) Patterns of heterozygosity (blue), a LROH (grey) and homozygous similarity (orange) are seen in 14_01223, 07_00242 and 16_00964 (green), and high heterozygosity in 16_00075 and 14_642 (red). All isolates were disomic for chromosome 36, except 14_00642 that was trisomic. The putative TSS inferred from *L. major* is at 1.63 Mb (black), corresponding to a recombination breakpoint in 14_01223 (middle). 07_00242 (top) and 16_00964 (second) had breakpoint at an inferred strand-switch region (SSR) at 1.42 Mb. (B) The inferred genetically distinct groups are represented by the *L. tropica* reference (yellow area) and non-reference groups (purple area). (C) The homozygous (x-axis) and heterozygous (y-axis) SNPs/Kb for all 22 samples for the 0–1.28 Mb region (top), 1.60–1.78 region (middle) and >1.8 Mb region (bottom).

all chromosome copies and possible accelerated mutation rates [49]. Consistent with this faster chromosomal substitution rate, the haploid *L. tropica* reference had high divergence at this chromosome (average across 22 samples 8.19±2.15 SNPs/Kb) compared to the other 35 chromosomes (5.01±0.66 SNPs/Kb, t = -34.8, p = 4.4x10^{-16}). This was due to a high rate of heterozygous SNPs (average 8.13±2.17) relative to the other 35 chromosomes (5.85±-0.55 SNPs/Kb, t = -36.6, p = 4.4x10^{-16}), but this was not evident for homozygous SNPs (0.06±0.06 vs 0.15±0.17 SNPs/Kb). The RDAF distribution of chromosome 31 of heterozygous SNPs was second lowest of the chromosomes (S7 Fig), suggesting more recombination resulting in consistent heterozygosity. The FastBAPS genetic group allocation was consistent with differing heterozygous SNP rates between the reference and non-reference groups, potentially indicating a lack of genetic exchange between these groups for this chromosome (Fig 4).

Chromosome 31 had sharp changes in heterozygosity at 220 Kb and 950 Kb in samples 15_02015 and 15_01620, and at 950 Kb in 15_02597 (for which chromosome 31 was pentasomic) (Fig 4).

In 15_01620, the major RDAF switched from a mode of 0.75 at <220 Kb to 0.5 at 220–950 Kb, before increasing to 0.75 at >950 Kb (Fig 4). In 15_02576, the major RDAF modes were 0.4 and 0.6 <950 Kb, followed by 0.6 at >950 Kb (Fig 4). 15_02597's RDAF had a major peak of 0.5 <950 Kb and a jump to 0.8 at >950 Kb (Fig 4). In 16_00075, the major RDAF peak was between 0.5 and 0.6 throughout (Fig 4). 15_02015's RDAF peaks were at 0.25 and 0.5 <220
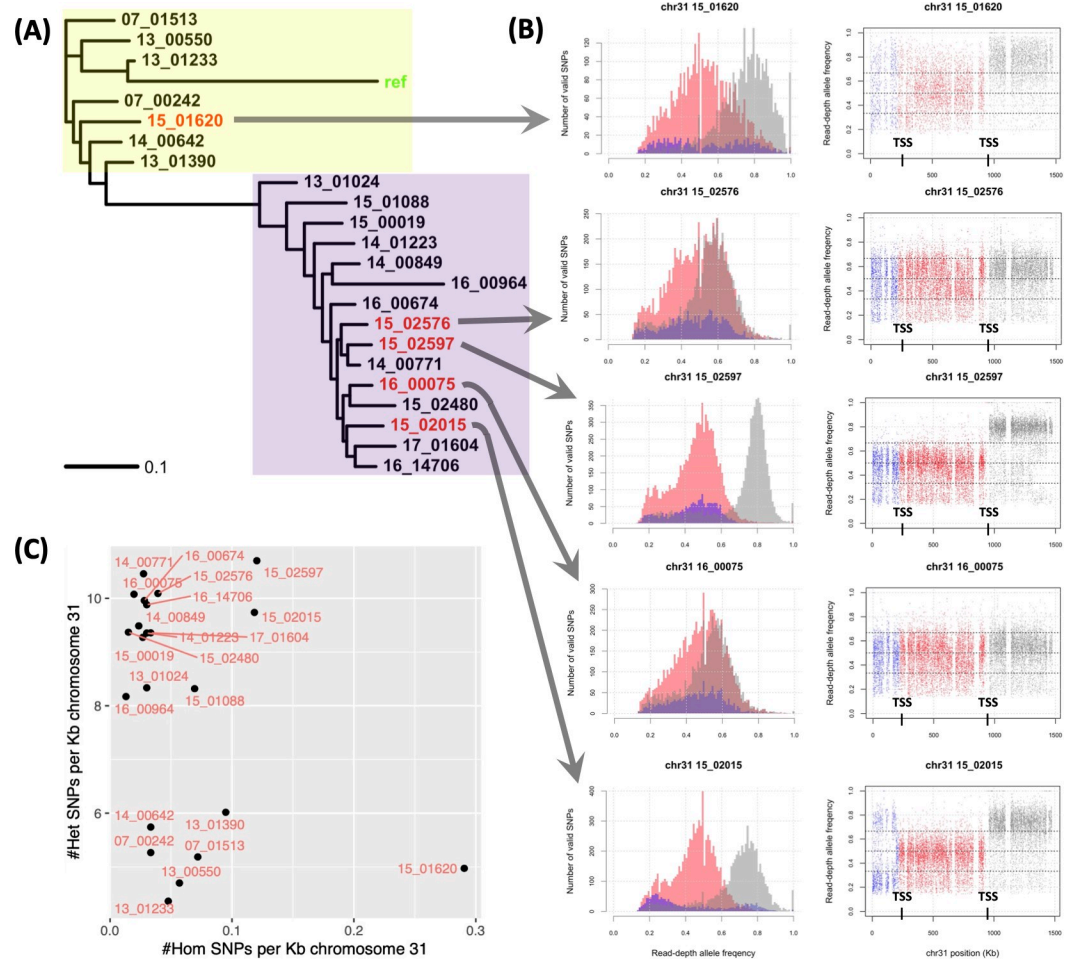
Fig 4. Heterozygosity was high and haplotype-specific on chromosome 31. (A) A rooted phylogeny constructed from SNPs at chromosome 31 showing a divergent *L. tropica* reference ("ref", green) due to a lack of heterozygous SNPs in this haploid genome. The inferred genetically distinct groups are represented by a group more related to the *L. tropica* reference (yellow area) and the non-reference group (purple area). (B) The read-depth allele frequency (RDAF) SNP densities (left) and distribution (right) across chromosome 31 (left) showed distinct patterns at the 5' end (<220 Kb, blue), middle (220–950 Kb, red) and 3' end (>950 Kb). 15_01620 (top) and 15_02015 (bottom) had recombination breakpoints at 220 and 950 Kb, coinciding with two putative TSSs inferred from experiments in *L. major* were at 220 and 950 Kb (black). 15_02597 (middle) also had a breakpoint at 950 Kb. 15_02576 (second) and 16_00075 (fourth) had no clear breakpoints. (C) The homozygous (x-axis) and heterozygous (y-axis) SNPs/Kb.

Kb, then 0.5 at 220–950 Kb, before 0.75 at >950 Kb (Fig 4). 220 Kb and 950 Kb are at TSSs containing acH3 marks, potentially matching TSSs inferred from experiments in *L. major*. These results demonstrate the high level of recombination at discrete breakpoints on this chromosome.

A geographic basis for unique ancestry and variation at chromosome 2

Sample 16_00964 from Iran, which also had mixed heterozygosity with putative novel ancestry at chromosome 36, also showed the same pattern on chromosome 29 at >440 Kb, and this was shared with sample 07_00242 (at >490 Kb) from Iran as well. Both had heterozygosity up to 440 (16_00964) or 490 (07_00242) Kb as did the other 20 samples, followed by a LROH from this point to the end of the chromosome at 1,520 Kb (Fig 5). This 440–490 Kb region was near
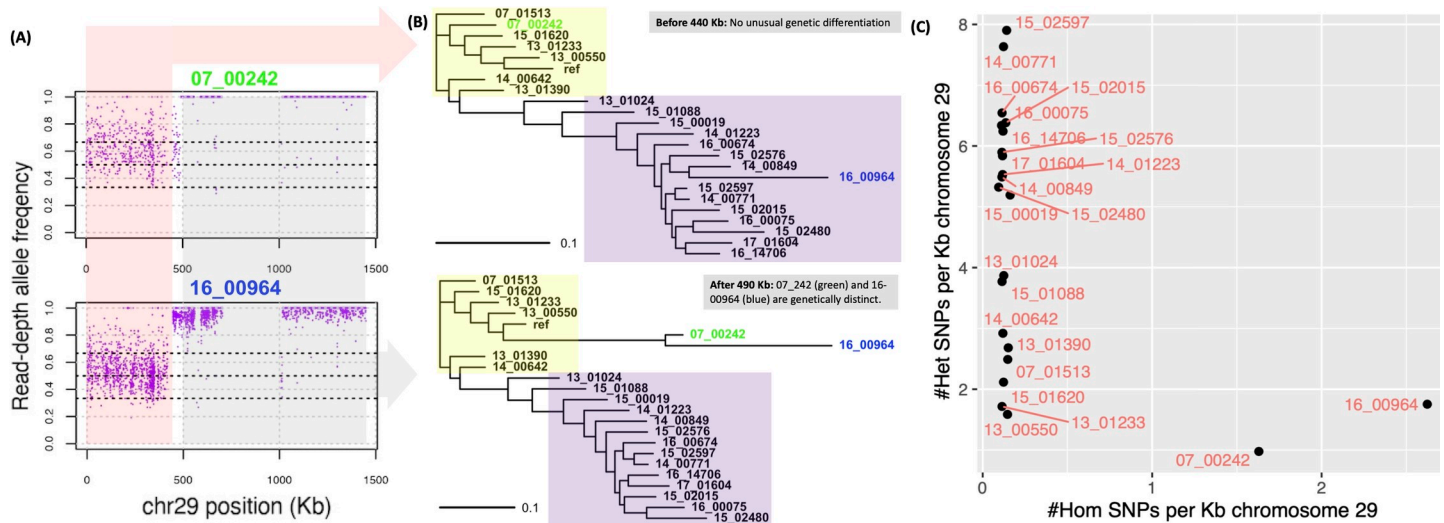
Fig 5. RDAF distributions (A) and phylogenies (B) constructed from SNPs at chromosome 29 from 0–440 Kb (pink RDAF, top phylogeny) and >490 Kb (grey RDAF, bottom phylogeny) showing the genetic relatedness of the 22 isolates with the *L. tropica* reference genome ("ref"). This showed unique segments of genetically distinct ancestries in 07_00242 (green) and 16_00964 (blue)—both came from patients originally from Iran. All samples were disomic for chromosome 29. The inferred genetically distinct groups are represented by the *L. tropica* reference (yellow area) and non-reference groups (purple area). (C) The homozygous (x-axis) and heterozygous (y-axis) SNPs per Kb for all 22 samples.

a TSS and a SSR. The genetic variation at >490 Kb in 16_00964 or 07_00242 was unlike the other samples and the reference genome, suggesting ancestry from an unsampled lineage ([Fig 5]). A similar picture of genetic exchange in another *L. donovani* lineage has been described near the region [40].

All three samples from Afghanistan (13_01233, 15_02480 and 16_00075) had 1.7-fold normalised average haploid read depth for chromosome 29 at 704–1,006 Kb (302 Kb total length), but the coverage was just 0.6 in the other 19 samples from Iran and Syria ([S8 Fig]). The rest of this chromosome was uniformly disomic in all samples (average depth 1.99±0.08), in line with the other chromosomes (average excluding chromosome 31, 2.12±0.33). This drop in read coverage was confirmed visually based on the read mapping distribution to the reference genome and again with the 13_00550 PacBio assembly ([S9 Fig]). This heterozygous deletion or contraction was present in the Iran- and Syria-linked samples from both the reference and non-reference genetic groups, and not the Afghanistan-linked samples, again from both reference (13_01233) and non-reference (15_02480 and 16_00075) groups ([Fig 1]).

Geographic structure associated with heterozygosity loss on chromosome 23

Like chromosomes 29 and 36, the region <250 Kb at chromosome 23 had a segment of ancestry that was distinct from the reference and non-reference patterns with high heterozygosity in five samples (all from Iran or Afghanistan) that formed their own genetic group in the FastBAPS population assignment ([S10 Fig]). This difference in ancestry was due to the high level of homozygous differentiation from the reference genome of the other 17 samples from Syria at <250 Kb, unlike the high heterozygosity seen in 07_00242 and 16_00964 (both Iran), and 13_01233, 15_02480 and 16_00075 (all Afghanistan) ([Fig 6]). Chromosome 23 had a higher density of homozygous SNPs/Kb (1.02±0.56) compared to the other 35 chromosomes (0.13 ±0.07 SNPs/Kb, t = -74.6, p = 4.4x10^{-16}) and had the lowest mean RDAF using heterozygous SNPs (0.43±0.06 per sample) of all the chromosomes (average of the other 35, 0.52±0.04) ([S7]
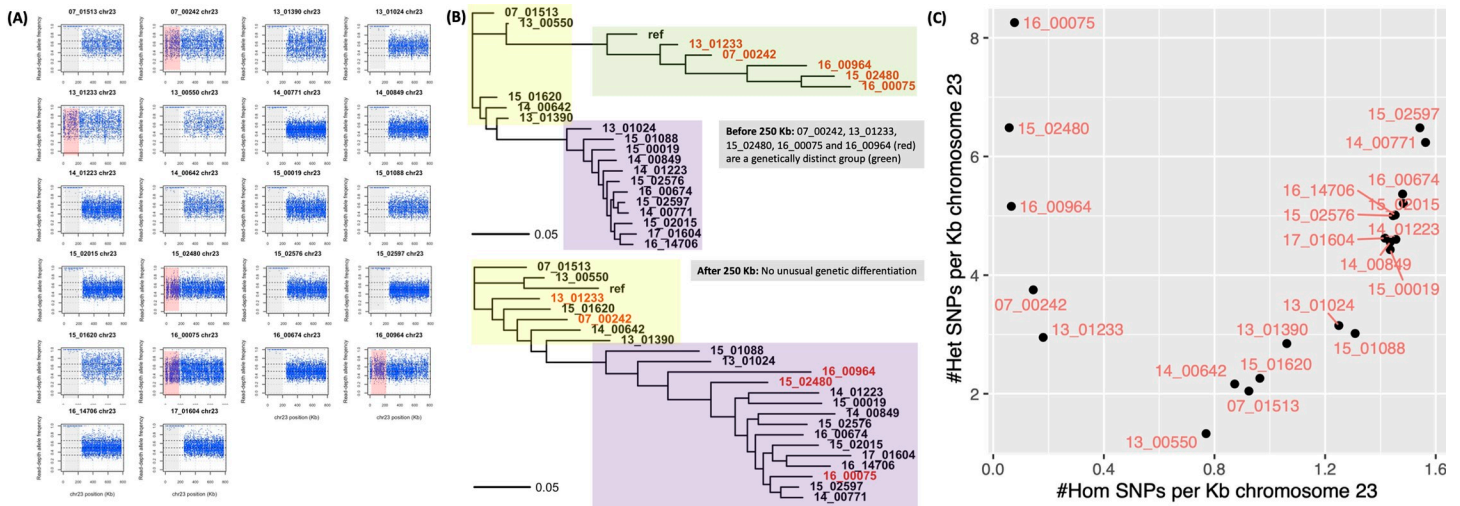
Fig 6. RDAF distributions (A) and phylogenies (B) constructed from SNPs at chromosome 23 at 0–250 Kb (grey and red in RDAF plots, top phylogeny) and >250 Kb (uncoloured RDAF, bottom phylogeny) showing the relatedness of the 22 isolates with the *L. tropica* reference genome ("ref"). This showed unique ancestries at chromosome 23 at 0–250 Kb with patterns related to the *L. tropica* reference in 07_00242, 13_01233, 15_02480, 16_00075 and 16_00964 (red in RDAF plots, red in phylogenies) and different patterns in the other 17 isolates. The inferred genetically distinct groups are represented by the *L. tropica* reference (yellow area) and non-reference groups (purple area). (C) The homozygous (x-axis) and heterozygous (y-axis) SNPs per Kb for all 22 samples.

Fig). This high SNP rate meant that this chromosome had 16.3% of all SNPs in each sample (795±343 vs 4,092±3,064 across the other 35 chromosomes). At >250 Kb, all samples conformed to their genome-wide pattern, such that 07_00242 and 13_01233 reverted to membership of the reference group, and 15_02480, 16_00075 and 16_00964 clustered with the non-reference group (Fig 6).

The near-uniform disomy of this chromosome in our isolates (average 2.15±0.27) and evidence of genetic drift from the high positive correlation of heterozygous and homozygous SNP densities in the 17 samples with LROHs suggested that recombination and somy changes were rare at this chromosome. We confirmed these results by read mapping the Ion Torrent library of 13_00550 to its own PacBio assembly to verify an absence of heterozygous SNPs before the 260 Kb position, followed by the heterozygosity >260Kb observed when mapping to the reference genome. This contrasted sharply with previous work on the *L. donovani* complex where chromosome 23 was typically trisomic with extensive diversity and encoded an amplification of the H-locus drug-resistance region [80].

Monosomy and trisomy on chromosome 10

Chromosome 10 was disomic in all isolates except 14_00642, which was monosomic at 20–250 Kb and approximately trisomic at <20 and >250 Kb (Fig 7). These results based on the normalised haploid depth from read mapping to the *L. tropica* reference genome were replicated in mapping to the contigs of a *de novo* Ion Torrent assembly of 14_00642 (Fig 7), and again when mapping to the PacBio 13_00550 assembly, and these unusual patterns were confirmed visually in IGV (S11 Fig). 14_00642 had a much higher rate of homozygous SNPs at chromosome 10 than the other samples (S12 Fig). The sub-telomeric regions of this chromosome could be amplified, coinciding with potential SSRs at 20 Kb and 520 Kb based on *L. major* experiments (Fig 7). Its RDAF distribution had peaks at ~0.67 at >250 Kb and at ~0.33 at >520 Kb, consistent with trisomy or possibly a mixed cell population. The switch from mono- to tri-somy was near a putative SSR at ~270 Kb, 5' of the inferred centromere at ~295–301 Kb
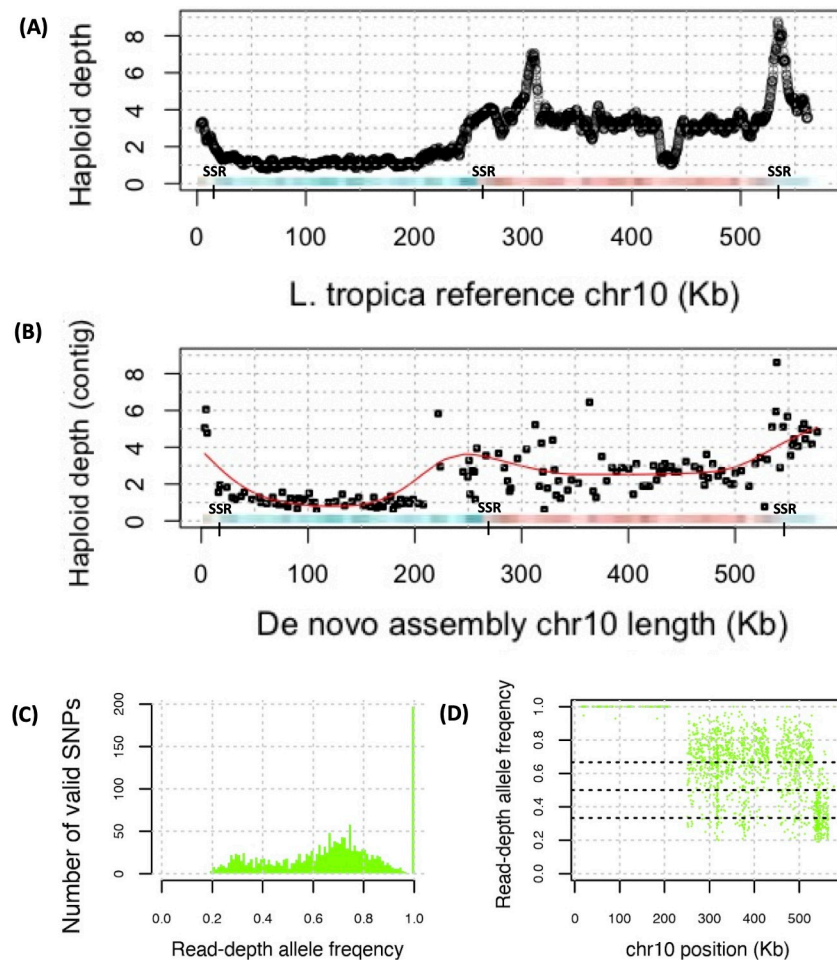
Fig 7. The normalised haploid depth (top) from read mapping to the *L. tropica* reference genome and for the contigs from a *de novo* assembly of 14_00642 (middle). Chromosome 10 potentially has three strand-switch regions (SSRs) inferred from experiments in *L. major* (red and blue panel). The lower panels show the numbers of valid SNPs (bottom left, green) and the RDAF for 14_00642.

https://doi.org/10.1371/journal.pntd.0010110.g007

[81] (Fig 7). 14_00642's pattern of low heterozygosity and LROHs was not in the other isolates except 15_02480, which had a LROH at >520 Kb, but had uniform disomy, like the other 20 samples (S12 Fig). The 230–250 Kb region contained numerous reference genome gaps and regions of low read mapping coverage, preventing clear delineation of a hypothetical break between the putative 5' chromosome 10.1 and 3' chromosome 10.2. Despite this, it is possible that this centromeric region delineates the formation of an acrocentric chromosome.

Aneuploidy as a mechanism for more allelic variation, recombination and adaptive paths

We found 17 mutations at 11 SNPs that were triallelic, such that two derived alleles were present. These were in 14 of the 22 samples, which had between four and eleven such multi-allelic SNPs each. The somy level of chromosomes with triallelic SNPs (4.32±0.39) was higher than that of chromosomes with biallelic SNPs (2.11±0.33, $p = 4.5\text{x}10^{-7}$). In addition to these unusual LROHs at chromosomes 10, 23, 29, and 36 above, we observed rare switches to homozygosity for chromosomes 2 in 14_01223 (entire chromosome, S3 Fig), 4 in 07_00242 (entire

chromosome, S13 Fig), 11 in 07_01513 (at >380 Kb, S14 Fig), 12 in 15_02480 (at >330 Kb, S15 Fig), 13 in 07_00242 and 16_00964 (at >530 Kb, S16 Fig), 14 in 14_00642 (at <70 Kb, S17 Fig), 17 in 07_00242 (at <80 Kb, S18 Fig), 22 in 07_00242 (entire chromosome, S19 Fig), 24 in 07_01513 (at <150 Kb, S20 Fig), 27 in 13_01390 (at <1.05 Mb, S21 Fig), 28 in 14_00771 (at <180 Kb) and 15_02480 (at <210 Kb, S22 Fig), 30 in 15_02015 (at <120 Kb, S23 Fig) and 33 in 07_00242 (at >1.2 Mb, S24 Fig). Furthermore, the most common changes in heterozygosity frequency for chromosomes 10, 23, 31 and 36 driven by recombination and (in some cases) somy changes were akin to less frequent changes on chromosomes 8 (at <110 Kb and >380 Kb) in 13_01233, 14_00642, 15_01620 and 16_00075 (S25 Fig), 22 (at <90 Kb and >460 Kb) in 14_00642 (S19 Fig), 24 (at <90 Kb and 200 Kb) in 14_00771 (S20 Fig), 25 (different small sections) in 14_00771 and 15_02597 (S26 Fig) and 27 (at >1.05 Mb) in 13_01390 (S21 Fig). Moreover, LROHs similar to those in chromosomes 23, 29 and 36 described above, associated with potential regions of ancestry different from the reference and non-reference groups, was observed in chromosomes 28 in 16_00964 (at <740 Kb, S22 Fig), 32 in 07_00242 (entire chromosome) and in 15_02015 (at <1.0 Mb, S27 Fig). This pervasive recombination was underpinned by the absence of a deviation from the genome-wide patterns of group clustering in the kDNA SNP patterns (S28 Fig).

Discussion

Here, we presented the genetic diversity and high degree of genomic variation within 22 isolates of *L. tropica* and found 301,659 SNPs across all samples, a number comparable to previous work [46]. We detected high heterozygosity and diverse LROHs, resulting in no clear correlation between the number of homozygous and heterozygous chromosomal SNPs per sample, in line with prior studies. This implied recombination and aneuploidy as key factors driving patchy genome-wide heterozygosity arising from older hybridisation events. In particular, chromosome 36 had shared patterns of heterozygosity followed by homozygous differentiation and then homozygous similarity, all on the same chromosome in 14_01223, 07_00242 and 16_00964. Our pattern of recombination breakpoints was similar to or exceeded rates of one cross-over per 1.5 Mb [32] or per 2.3 Mb [40], though an exact rate within *L. tropica* remains unclear. Across the genome, the extensive nature of the LROHs were indicative of regular recombination, and this pattern was present in both the main reference and non-reference genetic groups. These patterns suggested an increase somy allowed more recombination between chromosomes, a higher rate of derived allele accumulation, and hypothetically more diverse options following reversion to disomy associated with random loss of one chromosome copy.

Chromosome fission and fusion arise due to errors in chromosome replication and are rare in *Leishmania*. They tend to correlate with SSRs [82] that may be detected from histone H3 acetylation marks in *L. major* [55,83] and may preserve transcription of the PTUs. All except 14_00642's chromosome 10 were normal, and the 230–250 Kb region contained numerous reference genome gaps and regions of low read mapping coverage, preventing clear delineation of a hypothetical break between a putative 5' chromosome 10.1 and a 3' chromosome 10.2. Consequently, if a model of transient monosomy is excluded, then 50% of 14_00642's cells may have an intact disomic chromosome 10 and 50% may have a tetrasomic chromosome 10.2. Alternatively, all cells may have a disomic chromosome 10.2, and 50% may have an intact disomic chromosome 10 as well. Due to the effects of PCR during library preparation and the single-ended nature of these read libraries, they were insufficient to address subsequent questions on the location and sizes of the telomeric and centromeric DNA regions at new hypothetical chromosomes, though a variety of mechanisms exist to ensure cells can mitigate these chromosomal changes [84].

Telomeric amplification helps stabilise the genome during replication [85]. In *Leishmania*, the maintenance of telomeres occurs through rolling circle replication via extrachromosomal amplification, as in *Kluyveromyces lactis* [86,87] rather than telomeric loop formation [78]. And outside of the S cell cycle phase, DNA replication has been detected proximal to the chromosome telomeres, resembling a subtelomeric DNA synthesis activity [56]. Our isolates had extensive aneuploidy and higher heterozygosity than previously reported [46]. Recombination breakpoints coinciding with TSSs or SSRs were observed on numerous other chromosomes, which might affect DNA replication.

L. tropica likely has a higher capacity for interspecies mixing compared to other *Leishmania* and can create hybrids *in vivo* and *in vitro* [24,32,37,40,88]. *L. tropica* has a high efficiency of hybrid formation in co-infected sand flies and potentially greater capacity to generate mating-competent hybrids [32]. Genetic exchange occurs during reproduction by promastigotes in sand flies, and patterns of high and varied haplotype diversity were apparent in our results. This raises questions on the role of vector-species compatibility as a trigger for a sexual reproduction, and the potential for different sand flies to have varying microenvironments that differentially facilitate genetic exchange and hybrid generation. An important emerging question thus is the molecular basis of *L. tropica*'s broad vector compatibility, and how local environments mediate this [80,89].

Mosaic aneuploidy may originate through multiple mechanisms, not limited to meiotic nondisjunction, gene conversion [29], mitotic nondisjunction resulting in misallocating chromosomes [47], recombination-directed replication inferred from work on related parasites [55], and chromosomal replication followed by genome erosion [46]. To maintain the mosaic aneuploidy, Sterkers et al [30] argued for a parasexual reproduction, rather than a classical meiosis-like cycle, based on asymmetric chromosome allotments during mitosis. The distinctive heterozygosity blocks and aneuploidy among our isolates could be explained by either meiosis followed by selfing and chromosome copy number variation, or alternatively parasexual reproduction involving a tetraploid intermediate, or indeed both [88]. Recombination involving mobile genetic elements have also been suggested as a possible mechanism for the creation of mosaic aneuploidy [90].

Effect of long-term culturing of *Leishmania* and the environmental condition *in vitro* have previously been studied [91,92]. Structural variation, changes in ploidy [93] and altered gene dosage [47,94] has been observed in culture. Our isolates were cultured when diagnosed, before being stored at -156˚C and then re-cultured as promastigotes in axenic culture *in vitro* for two to six weeks before being DNA sequenced. Consequently, polymorphisms may have arisen during these steps and indeed some may have been lost. Moreover, although our study had the advantage of longer reads than typical Illumina runs, it lacked the information to resolve structural changes using paired read information and higher read depth would yield more precision in assessing copy number variation across chromosomes and subtle changes in heterozygosity. Notwithstanding our long read sequencing of one isolate, improving the quality of our reference genomes can spur new insights into regions with high structural variability and complex ancestry that may have been missed in this study.

Conclusion

The high diversity, frequent changes in heterozygosity and abundant aneuploidy in these 22 *L. tropica* isolates were consistent with genetic exchange, possibly by sexual or parasexual mechanisms. Different frequencies of recombination have been observed between different *Leishmania* populations [80]. *L. tropica*—*L. donovani* hybrids that have spread to geographically distant regions though diverse *Phlebotomomus spp.* by genetic exchanges to adapt to the vector

have been described [16,28,89]. It remains unclear if this is due to intrinsic differences in *Leishmania* or due to differences in vector species. What is clear is that *L. tropica* has adapted to several vector species, which seems to increase hybridization, and can produce new progeny with genetically highly similar or extremely distinct *Leishmania*. The diverse ancestries, mixing and existence of hybrids may help explain the challenges in treating CL and leishmaniaisis revidans caused by *L. tropica* in the Middle East, but further research needs to be carried out to better understand the correlations between genetic diversity in *Leishmania*, the differences among the vectors and treatment outcome.

Supporting information

S1 Table. The number of total, valid, and discarded sequence reads per sample, along with the numbers of candidate and valid SNPs per sample.
(TIF)

S1 Fig. The read coverage (A), mapping quality (MQ) (B), reverse reads (C) and forward reads (D) (all on x-axes) varied across the 22 samples (coloured dashed lines) compared to the number of SNPs called (y-axes).
(TIF)

S2 Fig. The numbers of homozygous (x-axis) and heterozygous (y-axis) chromosomal SNPs per sample.
(TIF)

S3 Fig. 14_01223 had evidence of near-homozygosity on chromosome 2 where it had 539 homozygous SNPs (>6 times more than all the other samples) and only 359 heterozygous SNPs (far fewer than the others).
(TIF)

S4 Fig. The chromosomes' (x-axis) distributions of their normalised haploid read depth per base (y-axis) for all 22 isolates.
(TIF)

S5 Fig. (A) Assignment of genetically distinct population using FastBAPS for SNPs at <1.28 Mb, 1.60–1.78 Mb, and > 1.80 Mb on chromosome 36 showing the genetic relatedness of the 22 isolates with the L. tropica reference genome ("ref", red group).
(TIF)

S6 Fig. The read-depth allele (RDAF) distributions SNPs at chromosome 36's 5' end (<1280 Kb, red), middle (1600–1780 Kb, blue) and 3' end (>1800 Kb, grey).
(TIF)

S7 Fig. The read-depth allele frequency (RDAF) levels for heterozygous SNPs (y-axis) across chromosomes (x-axis) shown as boxplots highlighting the interquartile range.
(TIF)

S8 Fig. Chromosome 29 had a region at 704–1,006 Kb (302 Kb in length) with low depth (y-axis, normalised to haploid).
(TIF)

S9 Fig. Visualisation of the reads mapped to the reference genome at chromosome 29 at 678–732 Kb (top) and at 977–1,031 Kb (bottom) showing no change in coverage in 15_020480 (middle) compared to 14_00642 (top) with the heterozygous deletion.
(TIF)

S10 Fig. Assignment of genetically distinct population using FastBAPs for SNPs at chromosome 23.
(TIF)

S11 Fig. The read coverage and heterozygosity visualised for 14_00642's chromosome 10 reads for bases 0–340 Kb (top) and 240–580 Kb (bottom) using IGV.
(TIF)

S12 Fig. The read depth in isolates 15_02480 (top) and 14_00642 (bottom) when reads were mapped to the L. tropica reference genome (A) and then to their own de novo genome assemblies (B).
(TIF)

S13 Fig. 07_00242 had homozygosity spanning the whole of chromosome 4 based on the read-depth allele frequency (RDAF) distribution (A) showing zero heterozygous SNPs and the RDAF across the chromosome showing minimal changes bar 720 homozygous SNPs.
(TIF)

S14 Fig. 07_01513 had evidence of heterozygosity followed by homozygosity >380 Kb on chromosome 11 where it had 652 homozygous (>7 times more than all the other samples).
(TIF)

S15 Fig. 15_02480 alone had a recombination breakpoint separating a heterozygous region at 0–330 on chromosome 12 from a homozygous one at >300 Kb.
(TIF)

S16 Fig. 07_00242 and 16_00964 had evidence of recombination breakpoints separating a homozygous region at >530 Kb on chromosome 13 from heterozygous regions 5' of this.
(TIF)

S17 Fig. 14_00642 had evidence of homozygosity at <70 Kb on chromosome 14 where it had 213 homozygous SNPs across the chromosome (90% more all the other samples), followed by heterozygosity >70 Kb.
(TIF)

S18 Fig. 07_00242 had homozygosity at <80 Kb on chromosome 17 following by heterozygosity.
(TIF)

S19 Fig. 07_00242 had homozygosity for all of chromosome 22.
(TIF)

S20 Fig. 07_01513 (A) and 14_00771 (B) had evidence of recombination breakpoints separating a homozygous region at <90 Kb in 14_00771 and <150 Kb in 07_01513 on chromosome 24 from heterozygous regions 3' of this.
(TIF)

S21 Fig. 13_01390 had evidence of quasi-homozygosity on chromosome 27 where it had 1,626 homozygous (>8 times more than all the other samples).
(TIF)

S22 Fig. 15_02480 (A), 14_00771 (B) and 16_00964 (C) had evidence of recombination breakpoints separating a homozygous region at <180 Kb in 14_00771, at <210 Kb in 15_02480, and at <740 Kb in 16–00964 on chromosome 28 from heterozygous regions 3' of this.
(TIF)

S23 Fig. 15_02015 had evidence of a homozygous region at <120 Kb on chromosome 30 where it had 479 homozygous (more than twice any other sample).
(TIF)

S24 Fig. 07_00242 had heterozygosity at <1.2 Mb on chromosome 33 following by mainly homozygosity >1.2 Mb.
(TIF)

S25 Fig. There was evidence of recombination breakpoints separating regions with a lower average read-depth allele frequency (RDAF) at 110–380 Kb from one with higher average RDAF at <110 Kb and >380 Kb on chromosome 8.
(TIF)

S26 Fig. 15_02597 (A) and 14_00771 (B) and had numerous recombination breakpoints separating short regions of homozygosity on chromosome 25 from heterozygous regions.
(TIF)

S27 Fig. 15_02015 (A) 07_00242 (B) and had regions of homozygosity on chromosome 32 spanning the whole chromosome for 07_00242 based on the read-depth allele frequency (RDAF) distribution (left) and the dearth of heterozygous SNPs (right).
(TIF)

S28 Fig. A co-phylogeny constructed from kDNA (left) and genome-wide (right) SNPs showing the relatedness of the 22 isolates.
(TIF)

Acknowledgments

Author Contributions

Conceptualization: Hedvig Glans, Maria Bradley, Björn Andersson, Tim Downing.

Data curation: Hedvig Glans.

Investigation: Hedvig Glans.

Methodology: Hedvig Glans, Erik Alm, Tim Downing.

Project administration: Hedvig Glans, Björn Andersson.

Resources: Hedvig Glans, Maria Lind Karlberg, Reza Advani, Tim Downing.

Software: Erik Alm, Tim Downing.

Supervision: Hedvig Glans, Maria Bradley, Björn Andersson, Tim Downing.

Visualization: Tim Downing.

Writing – original draft: Hedvig Glans, Björn Andersson, Tim Downing.

Writing – review & editing: Hedvig Glans, Maria Lind Karlberg, Reza Advani, Maria Bradley, Erik Alm, Björn Andersson, Tim Downing.

References

1. Alvar J, Velez ID, Bern C, Herrero M, Desjeux P, Cano J, et al. Leishmaniasis worldwide and global estimates of its incidence. PloS one. 2012; 7(5):e35671. https://doi.org/10.1371/journal.pone.0035671 PMID: 22693548

2. Gramiccia M, Gradoni L. The current status of zoonotic leishmaniases and approaches to disease control. International journal for parasitology. 2005; 35(11–12):1169–80. https://doi.org/10.1016/j.ijpara.2005.07.001 PMID: 16162348

3. Control of the leishmaniases. World Health Organization technical report series. 2010(949):xii–xiii, 1–186, back cover. PMID: 21485694

4. Ready PD. Leishmaniasis emergence in Europe. Eurosurveillance. 2010; 15(10):19505. PMID: 20403308

5. Peacock CS, Seeger K, Harris D, Murphy L, Ruiz JC, Quail MA, et al. Comparative genomic analysis of three Leishmania species that cause diverse human disease. Nature genetics. 2007; 39(7):839–47. https://doi.org/10.1038/ng2053 PMID: 17572675

6. Cunze S, Kochmann J, Koch LK, Hasselmann KJQ, Klimpel S. Leishmaniasis in Eurasia and Africa: geographical distribution of vector species and pathogens. Royal Society open science. 2019; 6 (5):190334. https://doi.org/10.1098/rsos.190334 PMID: 31218068

7. McDowell MA, Rafati S, Ramalho-Ortigao M, Ben Salah A. Leishmaniasis: Middle East and North Africa research and development priorities. PLoS neglected tropical diseases. 2011; 5(7):e1219. https://doi.org/10.1371/journal.pntd.0001219 PMID: 21814585

8. Magill AJ, Grögl M, Gasser RA Jr., Sun W, Oster CN. Visceral infection caused by Leishmania tropica in veterans of Operation Desert Storm. The New England journal of medicine. 1993; 328(19):1383–7. https://doi.org/10.1056/NEJM199305133281904 PMID: 8292114

9. Sacks DL, Kenney RT, Kreutzer RD, Jaffe CL, Gupta AK, Sharma MC, et al. Indian kala-azar caused by Leishmania tropica. Lancet (London, England). 1995; 345(8955):959–61. https://doi.org/10.1016/s0140-6736(95)90703-3 PMID: 7715298

10. Salloum T, Moussa R, Rahy R, Al Deek J, Khalifeh I, El Hajj R, et al. Expanded genome-wide comparisons give novel insights into population structure and genetic heterogeneity of Leishmania tropica complex. PLoS neglected tropical diseases. 2020; 14(9):e0008684. https://doi.org/10.1371/journal.pntd.0008684 PMID: 32946436

11. Akhoundi M, Kuhls K, Cannet A, Votypka J, Marty P, Delaunay P, et al. A Historical Overview of the Classification, Evolution, and Dispersion of Leishmania Parasites and Sandflies. PLoS neglected tropical diseases. 2016; 10(3):e0004349. https://doi.org/10.1371/journal.pntd.0004349 PMID: 26937644

12. Postigo JA. Leishmaniasis in the World Health Organization Eastern Mediterranean Region. International journal of antimicrobial agents. 2010; 36 Suppl 1:S62–5. https://doi.org/10.1016/j.ijantimicag.2010.06.023 PMID: 20728317

13. Hadighi R, Boucher P, Khamesipour A, Meamar A, Roy G, Ouellette M, et al. Glucantime-resistant Leishmania tropica isolated from Iranian patients with cutaneous leishmaniasis are sensitive to alternative antileishmania drugs. Parasitology research. 2007; 101(5):1319–22. https://doi.org/10.1007/s00436-007-0638-0 PMID: 17610079

14. Hadighi R, Mohebali M, Boucher P, Hajjaran H, Khamesipour A, Ouellette M. Unresponsiveness to Glucantime treatment in Iranian cutaneous leishmaniasis due to drug-resistant Leishmania tropica parasites. PLoS medicine. 2006; 3(5):e162. https://doi.org/10.1371/journal.pmed.0030162 PMID: 16605301

15. Rougeron V, De Meeûs T, Banuls A-L. A primer for Leishmania population genetic studies. Trends in parasitology. 2015; 31(2):52–9. https://doi.org/10.1016/j.pt.2014.12.001 PMID: 25592839

16. Volf P, Benkova I, Myskova J, Sadlova J, Campino L, Ravel C. Increased transmission potential of Leishmania major/Leishmania infantum hybrids. International journal for parasitology. 2007; 37(6):589–93. https://doi.org/10.1016/j.ijpara.2007.02.002 PMID: 17376453

17. Vaselek S, Dvorak V, Hlavackova K, Ayhan N, Halada P, Oguz G, et al. A survey of sand flies (Diptera, Phlebotominae) along recurrent transit routes in Serbia. Acta tropica. 2019; 197:105063. https://doi.org/10.1016/j.actatropica.2019.105063 PMID: 31207207

18. Svobodova M, Votypka J, Peckova J, Dvorak V, Nasereddin A, Baneth G, et al. Distinct transmission cycles of Leishmania tropica in 2 adjacent foci, Northern Israel. Emerging infectious diseases. 2006; 12 (12):1860. https://doi.org/10.3201/eid1212.060497 PMID: 17326936

19. Owino BO, Matoke-Muhia D, Alraey Y, Mwangi JM, Ingonga JM, Ngumbi PM, et al. Association of Phlebotomus guggisbergi with Leishmania major and Leishmania tropica in a complex transmission setting for cutaneous leishmaniasis in Gilgil, Nakuru county, Kenya. PLoS neglected tropical diseases. 2019; 13(10):e0007712. https://doi.org/10.1371/journal.pntd.0007712 PMID: 31626654

20. Vaselek S, Volf P. Experimental infection of Phlebotomus perniciosus and Phlebotomus tobbi with different Leishmania tropica strains. International journal for parasitology. 2019; 49(11):831–5. https://doi.org/10.1016/j.ijpara.2019.05.009 PMID: 31401063

21. Rassi Y, Sanei Dehkordi A, Oshaghi MA, Abai MR, Mohtarami F, Enayati A, et al. First report on natural infection of the Phlebotomus tobbi by Leishmania infantum in northwestern Iran. Experimental parasitology. 2012; 131(3):344–9. https://doi.org/10.1016/j.exppara.2012.04.020 PMID: 22609304

22. Seblova V, Myskova J, Hlavacova J, Votypka J, Antoniou M, Volf P. Natural hybrid of Leishmania infantum/L. donovani: development in Phlebotomus tobbi, P. perniciosus and Lutzomyia longipalpis and comparison with non-hybrid strains differing in tissue tropism. Parasites & vectors. 2015; 8(1):1–8. https://doi.org/10.1186/s13071-015-1217-3 PMID: 26608249

23. Sunter J, Gull K. Shape, form, function and Leishmania pathogenicity: from textbook descriptions to biological understanding. Open biology. 2017; 7(9). https://doi.org/10.1098/rsob.170165 PMID: 28903998

24. Inbar E, Akopyants NS, Charmoy M, Romano A, Lawyer P, Elnaiem DE, et al. The mating competence of geographically diverse Leishmania major strains in their natural and unnatural sand fly vectors. PLoS genetics. 2013; 9(7):e1003672. https://doi.org/10.1371/journal.pgen.1003672 PMID: 23935521

25. Kelly JM, Law JM, Chapman CJ, Van Eys GJ, Evans DA. Evidence of genetic recombination in Leishmania. Molecular and biochemical parasitology. 1991; 46(2):253–63. https://doi.org/10.1016/0166-6851(91)90049-c PMID: 1656255

26. Schwenkenbecher JM, Wirth T, Schnur LF, Jaffe CL, Schallig H, Al-Jawabreh A, et al. Microsatellite analysis reveals genetic structure of Leishmania tropica. International journal for parasitology. 2006; 36(2):237–46. https://doi.org/10.1016/j.ijpara.2005.09.010 PMID: 16307745

27. Ravel C, Cortes S, Pratlong F, Morio F, Dedet JP, Campino L. First report of genetic hybrids between two very divergent Leishmania species: Leishmania infantum and Leishmania major. International journal for parasitology. 2006; 36(13):1383–8. https://doi.org/10.1016/j.ijpara.2006.06.019 PMID: 16930606

28. Dujardin JC, Banuls AL, Llanos-Cuentas A, Alvarez E, DeDoncker S, Jacquet D, et al. Putative Leishmania hybrids in the Eastern Andean valley of Huanuco, Peru. Acta tropica. 1995; 59(4):293–307. https://doi.org/10.1016/0001-706x(95)00094-u PMID: 8533665

29. Akopyants NS, Kimblin N, Secundino N, Patrick R, Peters N, Lawyer P, et al. Demonstration of genetic exchange during cyclical development of Leishmania in the sand fly vector. Science (New York, NY). 2009; 324(5924):265–8. https://doi.org/10.1126/science.1169464 PMID: 19359589

30. Sterkers Y, Crobu L, Lachaud L, Pagès M, Bastien P. Parasexuality and mosaic aneuploidy in Leishmania: alternative genetics. Trends in parasitology. 2014; 30(9):429–35. https://doi.org/10.1016/j.pt.2014.07.002 PMID: 25073852

31. Gaunt MW, Yeo M, Frame IA, Stothard JR, Carrasco HJ, Taylor MC, et al. Mechanism of genetic exchange in American trypanosomes. Nature. 2003; 421(6926):936–9. https://doi.org/10.1038/nature01438 PMID: 12606999

32. Inbar E, Shaik J, Iantorno SA, Romano A, Nzelu CO, Owens K, et al. Whole genome sequencing of experimental hybrids supports meiosis-like sexual recombination in Leishmania. PLoS genetics. 2019; 15(5):e1008042. https://doi.org/10.1371/journal.pgen.1008042 PMID: 31091230

33. Lanotte G, Rioux JA. Cell fusion in Leishmania (Kinetoplastida, Trypanosomatidae). Comptes rendus de l'Academie des sciences Serie III, Sciences de la vie. 1990; 310(7):285–8. PMID: 2111197

34. Romano A, Inbar E, Debrabant A, Charmoy M, Lawyer P, Ribeiro-Gomes F, et al. Cross-species genetic exchange between visceral and cutaneous strains of Leishmania in the sand fly vector. Proceedings of the National Academy of Sciences of the United States of America. 2014; 111(47):16808–13. https://doi.org/10.1073/pnas.1415109111 PMID: 25385616

35. Schwabl P, Imamura H, Van den Broeck F, Costales JA, Maiguashca-Sánchez J, Miles MA, et al. Meiotic sex in Chagas disease parasite Trypanosoma cruzi. Nature communications. 2019; 10(1):3972. https://doi.org/10.1038/s41467-019-11771-z PMID: 31481692

36. Heitman J. Evolution of eukaryotic microbial pathogens via covert sexual reproduction. Cell host & microbe. 2010; 8(1):86–99. https://doi.org/10.1016/j.chom.2010.06.011 PMID: 20638645

37. Louradour I, Ferreira TR, Ghosh K, Shaik J, Sacks D. In Vitro Generation of Leishmania Hybrids. Cell reports. 2020; 31(2):107507. https://doi.org/10.1016/j.celrep.2020.03.071 PMID: 32294444

38. Gelanew T, Hailu A, Schőnian G, Lewis MD, Miles MA, Yeo M. Multilocus sequence and microsatellite identification of intra-specific hybrids and ancestor-like donors among natural Ethiopian isolates of

Leishmania donovani. International journal for parasitology. 2014; 44(10):751–7. https://doi.org/10.1016/j.ijpara.2014.05.008 PMID: 24995620

39. Chargui N, Amro A, Haouas N, Schönian G, Babba H, Schmidt S, et al. Population structure of Tunisian Leishmania infantum and evidence for the existence of hybrids and gene flow between genetically different populations. International journal for parasitology. 2009; 39(7):801–11. https://doi.org/10.1016/j.ijpara.2008.11.016 PMID: 19211023

40. Rogers MB, Downing T, Smith BA, Imamura H, Sanders M, Svobodova M, et al. Genomic confirmation of hybridisation and recent inbreeding in a vector-isolated Leishmania population. PLoS genetics. 2014; 10(1):e1004092. https://doi.org/10.1371/journal.pgen.1004092 PMID: 24453988

41. Odiwuor S, De Doncker S, Maes I, Dujardin JC, Van der Auwera G. Natural Leishmania donovani/Leishmania aethiopica hybrids identified from Ethiopia. Infection, genetics and evolution: journal of molecular epidemiology and evolutionary genetics in infectious diseases. 2011; 11(8):2113–8. https://doi.org/10.1016/j.meegid.2011.04.026 PMID: 21558020

42. Rougeron V, De Meeûs T, Kako Ouraga S, Hide M, Bañuls AL. "Everything you always wanted to know about sex (but were afraid to ask)" in Leishmania after two decades of laboratory and field analyses. PLoS pathogens. 2010; 6(8):e1001004. https://doi.org/10.1371/journal.ppat.1001004 PMID: 20808896

43. Dujardin JC, Bañuls AL, Victoir K, De Doncker S, Arevalo J, Llanos-Cuentas A, et al. From population to genome: ecogenetics of Leishmania (Viannia) braziliensis and L. (V.) peruviana. Annals of tropical medicine and parasitology. 1995; 89 Suppl 1:45–53. https://doi.org/10.1080/00034983.1995.11813014 PMID: 8745927

44. Sadlova J, Yeo M, Seblova V, Lewis MD, Mauricio I, Volf P, et al. Visualisation of Leishmania donovani fluorescent hybrids during early stage development in the sand fly vector. PloS one. 2011; 6(5). https://doi.org/10.1371/journal.pone.0019851 PMID: 21637755

45. Michaeli S. Trans-splicing in trypanosomes: machinery and its impact on the parasite transcriptome. Future microbiology. 2011; 6(4):459–74. https://doi.org/10.2217/fmb.11.20 PMID: 21526946

46. Iantorno SA, Durrant C, Khan A, Sanders MJ, Beverley SM, Warren WC, et al. Gene Expression in Leishmania Is Regulated Predominantly by Gene Dosage. mBio. 2017; 8(5). https://doi.org/10.1128/mBio.01393-17 PMID: 28900023

47. Rogers MB, Hilley JD, Dickens NJ, Wilkes J, Bates PA, Depledge DP, et al. Chromosome and gene copy number variation allow major structural change between species and strains of Leishmania. Genome research. 2011; 21(12):2129–42. https://doi.org/10.1101/gr.122945.111 PMID: 22038252

48. Leprohon P, Legare D, Raymond F, Madore E, Hardiman G, Corbeil J, et al. Gene expression modulation is associated with gene amplification, supernumerary chromosomes and chromosome loss in antimony-resistant Leishmania infantum. Nucleic acids research. 2009; 37(5):1387–99. https://doi.org/10.1093/nar/gkn1069 PMID: 19129236

49. Bussotti G, Piel L, Pescher P, Domagalska MA, Shanmugha Rajan K, Cohen-Chalamish S, et al. Genome instability drives epistatic adaptation in the human pathogen Leishmania. bioRxiv. 2021:2021.06.15.448517. https://doi.org/10.1073/pnas.2113744118 PMID: 34903666

50. Lachaud L, Bourgeois N, Kuk N, Morelle C, Crobu L, Merlin G, et al. Constitutive mosaic aneuploidy is a unique genetic feature widespread in the Leishmania genus. Microbes and infection. 2014; 16(1):61–6. https://doi.org/10.1016/j.micinf.2013.09.005 PMID: 24120456

51. Mannaert A, Downing T, Imamura H, Dujardin JC. Adaptive mechanisms in pathogens: universal aneuploidy in Leishmania. Trends in parasitology. 2012; 28(9):370–6. https://doi.org/10.1016/j.pt.2012.06.003 PMID: 22789456

52. Dumetz F, Imamura H, Sanders M, Seblova V, Myskova J, Pescher P, et al. Modulation of Aneuploidy in Leishmania donovani during Adaptation to Different In Vitro and In Vivo Environments and Its Impact on Gene Expression. mBio. 2017; 8(3). https://doi.org/10.1128/mBio.00599-17 PMID: 28536289

53. Clayton C, Shapira M. Post-transcriptional regulation of gene expression in trypanosomes and leishmanias. Molecular and biochemical parasitology. 2007; 156(2):93–101. https://doi.org/10.1016/j.molbiopara.2007.07.007 PMID: 17765983

54. Sterkers Y, Lachaud L, Bourgeois N, Crobu L, Bastien P, Pagès M. Novel insights into genome plasticity in Eukaryotes: mosaic aneuploidy in Leishmania. Molecular microbiology. 2012; 86(1):15–23. https://doi.org/10.1111/j.1365-2958.2012.08185.x PMID: 22857263

55. Marques CA, Dickens NJ, Paape D, Campbell SJ, McCulloch R. Genome-wide mapping reveals single-origin chromosome replication in Leishmania, a eukaryotic microbe. Genome biology. 2015; 16:230. https://doi.org/10.1186/s13059-015-0788-9 PMID: 26481451

56. Damasceno JD, Marques CA, Beraldi D, Crouch K, Lapsley C, Obonaga R, et al. Genome duplication in Leishmania major relies on persistent subtelomeric DNA replication. eLife. 2020;9. https://doi.org/10.7554/eLife.58030 PMID: 32897188

57. Myler PJ, Sisk E, McDonagh PD, Martinez-Calvillo S, Schnaufer A, Sunkin SM, et al. Genomic organization and gene function in Leishmania. Biochemical Society transactions. 2000; 28(5):527–31. https://doi.org/10.1042/bst0280527 PMID: 11044368

58. Martínez-Calvillo S, Nguyen D, Stuart K, Myler PJ. Transcription initiation and termination on Leishmania major chromosome 3. Eukaryotic cell. 2004; 3(2):506–17. https://doi.org/10.1128/EC.3.2.506-517.2004 PMID: 15075279

59. Wedel C, Förstner KU, Derr R, Siegel TN. GT-rich promoters can drive RNA pol II transcription and deposition of H2A.Z in African trypanosomes. The EMBO journal. 2017; 36(17):2581–94. https://doi.org/10.15252/embj.201695323 PMID: 28701485

60. Laffitte MN, Leprohon P, Papadopoulou B, Ouellette M. Plasticity of the Leishmania genome leading to gene copy number variations and drug resistance. F1000Research. 2016; 5:2350. https://doi.org/10.12688/f1000research.9218.1 PMID: 27703673

61. El-Sayed NM, Myler PJ, Blandin G, Berriman M, Crabtree J, Aggarwal G, et al. Comparative genomics of trypanosomatid parasitic protozoa. Science (New York, NY). 2005; 309(5733):404–9. https://doi.org/10.1126/science.1112181 PMID: 16020724

62. Martínez-Calvillo S, Yan S, Nguyen D, Fox M, Stuart K, Myler PJ. Transcription of Leishmania major Friedlin chromosome 1 initiates in both directions within a single region. Molecular cell. 2003; 11 (5):1291–9. https://doi.org/10.1016/s1097-2765(03)00143-6 PMID: 12769852

63. Krayter L, Bumb RA, Azmi K, Wuttke J, Malik MD, Schnur LF, et al. Multilocus microsatellite typing reveals a genetic relationship but, also, genetic differences between Indian strains of Leishmania tropica causing cutaneous leishmaniasis and those causing visceral leishmaniasis. Parasites & vectors. 2014; 7:123. https://doi.org/10.1186/1756-3305-7-123 PMID: 24666968

64. Nicolle C. Cultures des corps de Leishman isoles de la rate dans trois cas d'anemic sptenique infantile. Bull Soc Pathol Exot. 1908; 1:121.

65. Beser J, Hallström BM, Advani A, Andersson S, Östlund G, Winiecka-Krusnell J, et al. Improving the genotyping resolution of Cryptosporidium hominis subtype IbA10G2 using one step PCR-based amplicon sequencing. Infection, Genetics and Evolution. 2017; 55:297–304. https://doi.org/10.1016/j.meegid.2017.08.035 PMID: 28919550

66. Steinbiss S, Silva-Franco F, Brunk B, Foth B, Hertz-Fowler C, Berriman M, et al. Companion: a web server for annotation and analysis of parasite genomes. Nucleic acids research. 2016; 44(W1):W29–34. https://doi.org/10.1093/nar/gkw292 PMID: 27105845

67. Frith MC. A new repeat-masking method enables specific detection of homologous sequences. Nucleic acids research. 2011; 39(4):e23. https://doi.org/10.1093/nar/gkq1212 PMID: 21109538

68. Danecek P, Bonfield JK, Liddle J, Marshall J, Ohan V, Pollard MO, et al. Twelve years of SAMtools and BCFtools. GigaScience. 2021; 10(2). https://doi.org/10.1093/gigascience/giab008 PMID: 33590861

69. Li D, Liu C-M, Luo R, Sadakane K, Lam T-W. MEGAHIT: an ultra-fast single-node solution for large and complex metagenomics assembly via succinct de Bruijn graph. Bioinformatics. 2015; 31(10):1674–6. https://doi.org/10.1093/bioinformatics/btv033 PMID: 25609793

70. Van den Broeck F, Savill NJ, Imamura H, Sanders M, Maes I, Cooper S, et al. Ecological divergence and hybridization of Neotropical Leishmania parasites. Proceedings of the National Academy of Sciences. 2020; 117(40):25159–68. https://doi.org/10.1073/pnas.1920136117 PMID: 32958676

71. Assefa S, Keane TM, Otto TD, Newbold C, Berriman M. ABACAS: algorithm-based automatic contiguation of assembled sequences. Bioinformatics. 2009; 25(15):1968–9. https://doi.org/10.1093/bioinformatics/btp347 PMID: 19497936

72. Chin C-S, Alexander DH, Marks P, Klammer AA, Drake J, Heiner C, et al. Nonhybrid, finished microbial genome assemblies from long-read SMRT sequencing data. Nature methods. 2013; 10(6):563. https://doi.org/10.1038/nmeth.2474 PMID: 23644548

73. Stamatakis A. RAxML version 8: a tool for phylogenetic analysis and post-analysis of large phylogenies. Bioinformatics. 2014; 30(9):1312–3. https://doi.org/10.1093/bioinformatics/btu033 PMID: 24451623

74. Galili T. dendextend: an R package for visualizing, adjusting and comparing trees of hierarchical clustering. Bioinformatics. 2015; 31(22):3718–20. https://doi.org/10.1093/bioinformatics/btv428 PMID: 26209431

75. Tonkin-Hill G, Lees JA, Bentley SD, Frost SDW, Corander J. Fast hierarchical Bayesian analysis of population structure. Nucleic acids research. 2019; 47(11):5539–49. https://doi.org/10.1093/nar/gkz361 PMID: 31076776

76. Yu G. Using ggtree to Visualize Data on Tree-Like Structures. Curr Protoc Bioinformatics. 2020; 69(1): e96. https://doi.org/10.1002/cpbi.96 PMID: 32162851

77. Simpson L. The mitochondrial genome of kinetoplastid protozoa: genomic organization, transcription, replication, and evolution. Annual review of microbiology. 1987; 41:363–82. https://doi.org/10.1146/annurev.mi.41.100187.002051 PMID: 2825587

78. Bussotti G, Gouzelou E, Côrtes Boité M, Kherachi I, Harrat Z, Eddaikra N, et al. Leishmania Genome Dynamics during Environmental Adaptation Reveal Strain-Specific Differences in Gene Copy Number Variation, Karyotype Instability, and Telomeric Amplification. mBio. 2018; 9(6).

79. Domagalska MA, Imamura H, Sanders M, Van den Broeck F, Bhattarai NR, Vanaerschot M, et al. Genomes of Leishmania parasites directly sequenced from patients with visceral leishmaniasis in the Indian subcontinent. PLoS neglected tropical diseases. 2019; 13(12):e0007900. https://doi.org/10.1371/journal.pntd.0007900 PMID: 31830038

80. Franssen SU, Durrant C, Stark O, Moser B, Downing T, Imamura H, et al. Global genome diversity of the Leishmania donovani complex. eLife. 2020;9. https://doi.org/10.7554/eLife.51243 PMID: 32209228

81. Garcia-Silva MR, Sollelis L, MacPherson CR, Stanojcic S, Kuk N, Crobu L, et al. Identification of the centromeres of Leishmania major: revealing the hidden pieces. EMBO reports. 2017; 18(11):1968–77. https://doi.org/10.15252/embr.201744216 PMID: 28935715

82. Coughlan S, Mulhair P, Sanders M, Schonian G, Cotton JA, Downing T. The genome of Leishmania adleri from a mammalian host highlights chromosome fission in Sauroleishmania. Sci Rep. 2017; 7:43747. https://doi.org/10.1038/srep43747 PMID: 28256610

83. Thomas S, Green A, Sturm NR, Campbell DA, Myler PJ. Histone acetylations mark origins of polycistronic transcription in Leishmania major. BMC genomics. 2009; 10(1):1–15. https://doi.org/10.1186/1471-2164-10-152 PMID: 19356248

84. Perry J, Slater HR, Choo KA. Centric fission—simple and complex mechanisms. Chromosome Research. 2004; 12(6):627–40. https://doi.org/10.1023/B:CHRO.0000036594.38997.59 PMID: 15289668

85. de Lange T. T-loops and the origin of telomeres. Nature reviews Molecular cell biology. 2004; 5(4):323–9. https://doi.org/10.1038/nrm1359 PMID: 15071557

86. Natarajan S, McEachern MJ. Recombinational telomere elongation promoted by DNA circles. Molecular and cellular biology. 2002; 22(13):4512–21. https://doi.org/10.1128/MCB.22.13.4512-4521.2002 PMID: 12052861

87. Ubeda JM, Raymond F, Mukherjee A, Plourde M, Gingras H, Roy G, et al. Genome-wide stochastic adaptive DNA amplification at direct and inverted DNA repeats in the parasite Leishmania. PLoS biology. 2014; 12(5):e1001868. https://doi.org/10.1371/journal.pbio.1001868 PMID: 24844805

88. Cotton J, Durrant C, Franssen S, Gelanew T, Hailu A, Mateus D, et al. Genomic analysis of natural intra-specific hybrids among Ethiopian isolates of Leishmania donovani. BioRxiv. 2019:516211.

89. Lypaczewski P, Hoshizaki J, Zhang WW, McCall LI, Torcivia-Rodriguez J, Simonyan V, et al. A complete Leishmania donovani reference genome identifies novel genetic variations associated with virulence. Sci Rep. 2018; 8(1):16549. https://doi.org/10.1038/s41598-018-34812-x PMID: 30409989

90. Llanes A, Restrepo CM, Del Vecchio G, Anguizola FJ, Lleonart R. The genome of Leishmania panamensis: insights into genomics of the L. (Viannia) subgenus. Sci Rep. 2015; 5:8550. https://doi.org/10.1038/srep08550 PMID: 25707621

91. Dey T, Afrin F, Anam K, Ali N. Infectivity and virulence of Leishmania donovani promastigotes: a role for media, source, and strain of parasite. The Journal of eukaryotic microbiology. 2002; 49(4):270–4. https://doi.org/10.1111/j.1550-7408.2002.tb00369.x PMID: 12188216

92. Segovia M, Artero JM, Mellado E, Chance ML. Effects of long-term in vitro cultivation on the virulence of cloned lines of Leishmania major promastigotes. Annals of tropical medicine and parasitology. 1992; 86 (4):347–54. https://doi.org/10.1080/00034983.1992.11812677 PMID: 1463354

93. Sterkers Y, Lachaud L, Crobu L, Bastien P, Pages M. FISH analysis reveals aneuploidy and continual generation of chromosomal mosaicism in Leishmania major. Cellular microbiology. 2011; 13(2):274–83. https://doi.org/10.1111/j.1462-5822.2010.01534.x PMID: 20964798

94. Downing T, Imamura H, Decuypere S, Clark TG, Coombs GH, Cotton JA, et al. Whole genome sequencing of multiple Leishmania donovani clinical isolates provides insights into population structure and mechanisms of drug resistance. Genome research. 2011; 21(12):2143–56. https://doi.org/10.1101/gr.123430.111 PMID: 22038251